An improved measurement model for target tracking under measurement origin uncertainty

VIJI PAUL PANAKKAL
RAJBABU VELMURUGAN

Single-target tracking using a standard Kalman filter with fixed measurement noise covariance will be effective if the target originated measurement is known. Under measurement origin uncertainty (MOU) the target state is updated in a probabilistic data association (PDA) framework using the set of measurements obtained inside a validation region (gate region). This paper develops a model for validated measurements using a conventional target originated measurement model and a model for measurements with uncertain origin. Using the developed model for validated measurements the measurement noise covariance under measurement origin uncertainty (MOU) is estimated. With this model the multiplicative scalar information reduction factor (IRF) in the computation of Cramér-Rao lower bound (CRLB) with MOU is shown to be due to an additive term in the measurement noise covariance. This additive term is used in the probabilistic data association (PDA) filter for computing the spread of innovation. This leads to a modified measurement noise covariance, innovation covariance and Kalman filter gain resulting in an adaptive iterative PDA (Iter-PDA) filter. Improvements obtained using the proposed approach are demonstrated through Monte Carlo (MC) simulations by comparing with PDA and CRLB. The consistency of the modified filter is checked and found to be within the acceptable limits.

Manuscript received October 13, 2014; revised April 2, 2015; released for publication July 28, 2015.

Refereeing of this contribution was handled by Huimin Chen.

Authors' addresses: V. Panakkal, Central Research Laboratory, Bharat Electronics Ltd., Bangalore, India (e-mail: vijipaulp@bel.co.in). R. Velmurugan, Dept. of Electrical Engineering, Indian Institute of Technology, Bombay, Mumbai, India (e-mail: rajbabu@ee.iitb.ac.in).

1557-6418/15/$17.00

1. INTRODUCTION

In surveillance systems, measurements can be due to targets of interest, clutter or false alarms. Target tracking in such conditions suffers from measurement origin uncertainty (MOU) in addition to measurement noise. Multiple hypotheses tracking (MHT), the optimal approach for tracking under MOU, [1], [2], uses all measurements $\mathbf{Z}^k$ up to time k for data association. The issue with MHT is the maintenance of exponentially increasing number of hypotheses with time [1]. MHT uses pruning and merging of hypotheses to limit the Gaussian components [3], [4]. Sub-optimal approaches such as probabilistic data association (PDA) use only the measurements $\mathbf{Z}(k)$ obtained at instant k for updating the predicted target state $\hat{\mathbf{x}}_i(k \mid k-1)$. Because of the reduced computational effort compared to the optimal approach and due to its robustness towards clutter and missed detection (measurement) PDA is widely used for tracking in clutter [5], [6]. Earlier work exploring different aspects of using PDA in target tracking such as, consistency, maneuver, track initiation-deletion and track bias have appeared in [7], [8], [9], [10], [11]. In this paper the focus is on improving the estimation accuracy under MOU by modeling the uncertainty associated with measurement origin.

PDA uses all the measurements inside a gate area around the predicted state known as validated measurements for state update using the Kalman filter framework. Hence, the posterior state error covariance of the Kalman filter is increased depending on the measurement origin uncertainty. The gate size is determined using the innovation covariance computed using the prediction error covariance and measurement noise covariance. As the state update progresses the filter used in state update attains steady state and the prediction error covariance in Kalman filter reduces. Therefore, for time index $k = 1, 2, 3$ the gate size computed using the innovation covariance reduces as shown in Fig. 1. The innovation covariance is also used in PDA filter for computing the measurement-to-track association hypotheses probability. In PDA filter, the Kalman filter gain and the innovation covariance corresponding to time instant k are computed using the parameters available at time $k-1$, i.e., without using measurements from kth instant. The proposed approach in this paper uses measurements from kth instant to compute innovation covariance and Kalman filter gain.

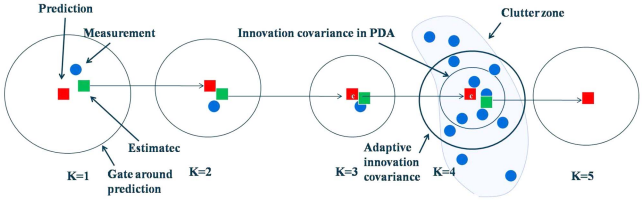

Fig. 1. Instantaneous adaptability of data association filter in clutter and clutter free zones.

In practice targets may move in clutter or clutter free zones and the tracking algorithm should adapt to the situation. As shown in Fig. 1, for time index $k = 4$ the target enters a clutter zone and the pre-computed innovation covariance does not anticipate a clutter environment. The PDA filter increases the posterior error covariance and anticipates such a situation for the next time instant at $k = 5$. The standard PDA implementations provided in [5], [6], [12], [13] lack the instantaneous adaptability to measurement origin uncertainty. The adaptability of PDA filter during target maneuver is addressed in [14] by scaling the process noise covariance using the available data at current time k. For bearings-only tracking the gain of the extended Kalman filter is modified in [15] for better handling of target maneuver. In the proposed approach, the innovation covariance is adapted instantaneously so that better measurement-to-track association hypotheses probability is obtained. Using the modified innovation covariance the Kalman filter gain with MOU is computed and used for state error covariance update. The innovation covariance is made adaptive by computing the modified measurement noise covariance representing the MOU in addition to the known measurement noise variance.

The method developed in this paper improves the target state estimation accuracy by adaptively adjusting the filter parameters used in state estimation. In the smoothed PDA filter [16], the estimation accuracy of the PDA filter is improved by using measurements from the future. The prior estimates such as predicted target state and innovation covariance can be improved using the smoothed PDA, but with increased computational cost due to the usage of measurements from multiple time instants. For the case of finite resolution sensors the estimation accuracy has been improved compared to PDA in [17] for static and dynamic clutter pattern. In the limiting case of infinite resolution sensors the approach in [17] gives similar estimation accuracy as PDA. In this paper the objective is to model the origin uncertainty and to improve the estimation accuracy compared to PDA even in the case of measurements obtained from sensors having infinite resolution. The estimation accuracy for closely moving targets are improved in iterative JPDA (Iter-JPDA) compared to JPDA by computing better measurement-to-track association probabilities [18], [19] using measurements from the current time frame. The approach presented here also improves the estimation accuracy using measurements from the current time frame. In [20] improved estimation accuracy in the PDA frame work has been obtained by modifying the data association probability with an assumption that the target originated measurements will always be closer to the predicted measurements. The approach developed in this paper improves estimation accuracy through better filter parameters obtained by modeling the measurement origin uncertainty. For the case of non-parametric tracking, a measurement sparsity estimation approach is developed in [21]. Compared to conventional track oriented clutter density estimation the sparsity estimation approach in [21] reports improved track confirmation rate, but the approach does not report estimation accuracy improvements. In parametric form the proposed approach in this paper assumes the spatial density of clutter measurements is known a priori, as in the case of parametric PDA, and assumes that the number of clutter measurements follow a Poisson distribution. In non-parametric form the Poisson parameter is replaced with sample spatial density as in PDA filter.

We compare the mean square error obtained using the proposed approach with the Cramér-Rao lower bound (CRLB) [22]. The CRLB for the unknown parameter estimation is given by the Fisher information matrix (FIM) [23]. The CRLB for a linear dynamic system in the presence of additive white Gaussian noise and MOU has been derived in [9], [24] and observed that a scalar information reduction factor (IRF) exists due to MOU. The sufficient condition for the existence of a scalar IRF in MOU and its wide application is shown in [25], [26]. The exact computation of CRLB with MOU requires higher order integrals to obtain the IRF [9], [24]. A recursive form of CRLB obeying matrix Riccati-like expression is obtained in [27], [28] with an exception that the measurement noise covariance term is multiplied by an IRF. A simplified recursive expression for CRLB is shown in [29], but still requires evaluation of higher order integrals. The tabulated values of IRF given in [27], [30] can be used as an approximation, but for a fixed process and measurement noise ($\mathbf{Q}$ and $\mathbf{R}$) along with gate size γ. In this paper the information matrix used for the computation of CRLB for linear Gaussian case with MOU has been computed using the modified measurement noise covariance in a recursive form. The derived expression for scalar IRF can be evaluated for any $\mathbf{Q}$, $\mathbf{R}$ and γ and avoids evaluation of higher order integrals.

The main contribution of this paper is in providing a model for validated measurements to carry out improved data association for target tracking in clutter. Compared to the target originated measurement model the developed model for validated measurements handles the measurement origin uncertainty (MOU). Using the proposed model for validated measurements the adaptive measurement noise covariance in target tracking with MOU is computed. With this adaptive measurement noise covariance other filter parameters are modified and improved target state estimates are obtained. Another contribution of this paper is a method to compute the information reduction factor (IRF) with Monte Carlo (MC) simulations. Using this IRF the CRLB with MOU is computed and the performance of the proposed approach is compared.

The outline of this paper is as follows. In Section 2 we discuss the standard PDA based estimation process for comparison with the proposed approach. The proposed measurement model for validated measurements

to handle MOU is developed in Section 3. Using this measurement model, the modified innovation covariance and Kalman filter gain can be computed. The PDA filter using the proposed model becomes iterative because of the dependency between measurement-to-track association hypothesis probability and the innovation covariance. In Section 4, the recursive form of information matrix update with MOU has been developed. Here we also show that the scalar multiplicative IRF is due to an additive term in the measurement noise covariance computed with MOU. Section 5 gives the simulation results and compares the root mean-square positional error. The filter consistency test results and the variation of IRF for various $\mathbf{Q}$, $\mathbf{R}$ and λ are also provided. Section 6 provides the conclusion.

2. TARGET STATE ESTIMATION USING PDA

Consider the target state transition and measurement model of the form

$$\mathbf{x}_i(k+1) = \mathbf{F}\mathbf{x}_i(k) + \mathbf{w}(k), \tag{1}$$

$$\mathbf{z}_i(k) = \mathbf{H}\mathbf{x}_i(k) + \mathbf{v}(k), \tag{2}$$

where k is the time index, $\mathbf{x}_i$ is a state vector of target i, $\mathbf{z}_i$ is the measurement vector, $\mathbf{w}$ and $\mathbf{v}$ are zero mean Gaussian noise vectors with covariance $\mathbf{Q}$ and $\mathbf{R}$, respectively. The measurements obtained inside a gate area around the predicted state is referred as validated measurements. The validated measurement set $\mathbf{Z}(k) = \{\mathbf{z}_j(k)\}_{j=1:m_k}$ obtained at kth scan consist of m_k number of measurements and $\mathbf{Z}^k = \{\mathbf{Z}(k)\}$ denotes the cumulative set of measurements up to time k. Among the set $\{\mathbf{z}_j(k)\}_{j=1:m_k}$ the index of target originated measurement is unknown and this causes the measurement origin uncertainty (MOU). The state transition matrix $\mathbf{F}$ and observation matrix $\mathbf{H}$ are assumed to be known. The predicted measurement is obtained from the predicted target state as $\hat{\mathbf{z}}_i(k \mid k-1) = \mathbf{H}\hat{\mathbf{x}}_i(k \mid k-1)$. The error of the predicted measurement is

$$\nu_i(k) = \mathbf{z}_i(k) - \hat{\mathbf{z}}_i(k \mid k-1),$$

and the corresponding innovation covariance is

$$\mathbf{S}_i(k) = E[\nu_i(k)\nu_i^T(k)]. \tag{3}$$

For single target tracking with measurement origin uncertainty, the joint association hypothesis is defined as

$$\mathbf{A}(j) = \begin{cases} j = 1 : m_k, \mathbf{z}_j(k) \text{ is associated with target and all other measurements are assumed to be from clutter.} \\ j = 0, \text{ No measurement is associated with target, all measurements are assumed to be from clutter.} \end{cases} \tag{4}$$

Measurement index $j = 0$ indicates no validated measurement is used for association. Therefore, $\mathbf{A}(0)$ indicates track is associated with predicted measurement $\hat{\mathbf{z}}(k \mid k-1)$. There are m_k number of measurements available at scan k and only one measurement is associated with track. Conventional PDA approach assumes the associated measurement to be target originated. The set of all validated association hypotheses are denoted as $\mathbf{A} = \{\mathbf{A}(j)\}_{j=0:m_k}$.

The measurements falling in the validation region $V(\gamma)$ are only considered for forming the association configuration. Validation region is a region around the predicted target state where the measurements will be available with high probability. The measurements inside the validation region satisfy the condition

$$V_k(\gamma) = [\mathbf{z} : \nu_j(k)\mathbf{S}_i^{-1}(k)\nu_j(k)^T \leq \gamma] \tag{5}$$

where γ is a parameter to control the validation (gate) region and the set of validated measurements at time k is denoted as $\mathbf{Z}(k) = \{\mathbf{z}_j(k)\}_{j=1:m_k}$. The probability of the hypothesis $\mathbf{A}(j)$ is computed in PDA as

$$\begin{aligned} \beta_j &= p(\mathbf{A}(j) \mid \mathbf{Z}^k) = p(\mathbf{A}(j) \mid \mathbf{Z}(k), m_k, \mathbf{Z}^{k-1}), \\ &= \frac{1}{c} p(\mathbf{Z}(k) \mid \mathbf{A}(j), m_k, \mathbf{Z}^{k-1}) p(\mathbf{A}(j) \mid m_k, \mathbf{Z}^{k-1}), \\ &= \frac{1}{c} p(\mathbf{Z}(k) \mid \mathbf{A}(j), m_k, \mathbf{Z}^{k-1}) p(\mathbf{A}(j) \mid m_k), \end{aligned} \tag{6}$$

where c is a normalizing constant. The conditioning of $\mathbf{A}(j)$ on $\mathbf{Z}^{k-1}$ is considered irrelevant and so the prior for data association $p(\mathbf{A}(j))$ is uniform in PDA [12]. Hence, the probability of association hypotheses unconditioned (conditioned only on number of measurements) with previous measurements is computed in (6). Because of the un-conditioning of $\mathbf{A}(j)$ with prior measurements the proposed approach computes the measurement likelihood using innovation covariance unconditioned with any data association hypothesis. In the context of parameter estimation accounting model selection uncertainty the unconditional covariance is computed in [31]. The unconditional covariance improves the precision in estimates by accounting the uncertainty about what model to use [31]. In target tracking under MOU the data association hypothesis $\mathbf{A}(j)$ assumes measurement $\mathbf{z}_j$ is originated from target. In the proposed approach the unconditional covariance accounts the uncertainty in $\mathbf{A}(j)$ and improves the estimation accuracy. The likelihood function of target originated measurement $\mathbf{z}_j(k)$ is computed in PDA assuming a Gaussian density with mean $\mathbf{H}\hat{\mathbf{x}}_i(k \mid k-1)$ and variance $\mathbf{S}_i(k)$, i.e. [12]

$$p(\mathbf{Z}(k) \mid \mathbf{A}(j), \mathbf{Z}^{k-1}) = \begin{cases} V_k^{-m_k+1} P_G^{-1} \mathcal{N}(\mathbf{z}_j(k); \mathbf{H}\hat{\mathbf{x}}_i(k \mid k-1), \mathbf{S}_i(k)), \\ \qquad j = 1, \ldots, m_k. \\ V_k^{-m_k} \quad j = 0. \end{cases} \tag{7}$$

where V_k is the volume of the validation region defined as

$$V_k = c_{n_z} \gamma^{n_z/2} |\mathbf{S}_i(k)|^{1/2}, \tag{8}$$

where n_z is the dimension of measurement (simulations carried out in this paper are with $n_z = 2$) and c_{n_z}

is the volume of the n_z dimensional unit hypersphere, and $c_2 = \pi$. In contrast to PDA, the proposed approach computes the likelihood given in (7) using a modified innovation covariance $\mathbf{S}_i^{\theta}(k)$, where the term $\mathbf{S}_i^{\theta}(k)$ is computed in the proposed approach as unconditional innovation covariance [31]. PDA uses $\mathbf{S}_i(k)$ in (7) assuming measurement $\mathbf{z}_j(k)$ is target originated. In the proposed approach the modified innovation covariance $\mathbf{S}_i^{\theta}(k)$ is computed using the modified measurement error covariance $\mathbf{R}_i^{\theta}(k)$.

2.1 Kalman filter

In the standard Kalman filter for tracking without MOU the prediction and update of error covariance matrices can be summarized as [32], [33]

$$\mathbf{P}_i(k \mid k-1) = \mathbf{F}\mathbf{P}_i(k-1)\mathbf{F}^T + \mathbf{Q}_i, \tag{9}$$

$$\begin{aligned}\mathbf{P}_i^*(k \mid k) = (\mathbf{I} - \mathbf{K}_i(k)\mathbf{H})\mathbf{P}_i(k \mid k-1)(\mathbf{I} - \mathbf{K}_i(k)\mathbf{H})^T \\ + \mathbf{K}_i(k)\mathbf{R}\mathbf{K}_i(k)^T,\end{aligned} \tag{10}$$

where $\mathbf{P}_i^*(k \mid k)$ denote posterior state error covariance without measurement origin uncertainty. The innovation covariance is computed as

$$\mathbf{S}_i(k) = \mathbf{H}\mathbf{P}_i(k \mid k-1)\mathbf{H}^T + \mathbf{R}. \tag{11}$$

The Kalman gain $\mathbf{K}_i(k)$ is computed as

$$\mathbf{K}_i(k) = \mathbf{P}_i(k \mid k-1)\mathbf{H}^T\mathbf{S}_i^{-1}(k). \tag{12}$$

The updated state estimate is obtained as

$$\tilde{\mathbf{x}}_i(k \mid k) = \hat{\mathbf{x}}_i(k \mid k-1) + \mathbf{K}_i(k)\nu_i(k). \tag{13}$$

In standard Kalman filter, the measurement originates from the known target, hence

$$\nu_i(k) = \mathbf{z}_i(k) - \mathbf{H}\hat{\mathbf{x}}_i(k \mid k-1),$$

can be computed without ambiguity.

2.2 Estimation with measurement origin uncertainty (MOU)

In most of the existing approaches to handle measurement origin uncertainty, the posterior target state is obtained as the conditional mean [5] by averaging over all valid association hypotheses. The conditional mean is obtained as the minimum mean square estimate (MMSE) [12]

$$\begin{aligned}\tilde{\mathbf{x}}_i^{(MMSE)}(k \mid k) &= E[\mathbf{x}_i(k) \mid \mathbf{Z}^k] \\ &= E[E[\mathbf{x}_i(k) \mid \mathbf{A}, \mathbf{Z}^k] \mid \mathbf{Z}^k] \\ &= \sum_{j=0:m_k} E[\mathbf{x}_i(k) \mid \mathbf{A}(j), \mathbf{Z}^k] P(\mathbf{A}(j) \mid \mathbf{Z}^k) \\ &= \sum_{j=0:m_k} E[\mathbf{x}_i(k) \mid \mathbf{A}(j), \mathbf{Z}^k]\beta_j.\end{aligned} \tag{14}$$

The term $\beta_j = p(\mathbf{A}(j) \mid \mathbf{Z}^k)$ is computed as [2], [12]

$$\beta_j = \begin{cases} \dfrac{b}{b + \sum_{j=1}^{m_k} e_j}, & j = 0 \text{ no valid measurement}, \\ \dfrac{e_j}{b + \sum_{j=1}^{m_k} e_j}, & 1 \le j \le m_k. \end{cases} \tag{15}$$

PDA filter in parametric form assumes the number of clutter measurements are obtained from Poisson model defined with parameter λ, where λ is the spatial density of false measurements. Parametric PDA filter computes b and e_j as follows

$$\begin{aligned} b &= \lambda\sqrt{2\pi|\mathbf{S}(k)|}\left(\frac{1 - P_d P_G}{P_d}\right), \\ e_j &= \exp(-0.5\nu_j^T(k)\mathbf{S}^{-1}(k)\nu_j(k)), \end{aligned} \tag{16}$$

where $|.|$ denotes the determinant, and P_d is the probability of detection and P_G is the probability of measurement falling inside the gate. In non-parametric form the Poisson parameter λ is replaced with sample spatial density $\lambda = m_k/V_k$ as the clutter density.

The proposed approach computes b and e_j using (16) by replacing $\mathbf{S}_i(k)$ with a modified innovation covariance $\mathbf{S}_i^{\theta}(k)$ to account for the measurement origin uncertainty. Less than unity value for β_j suggests that the origin of jth validated measurement is uncertain. The term $\tilde{\mathbf{x}}_i^{(j)}(k \mid k) = E[\mathbf{x}_i(k) \mid \mathbf{A}(j), \mathbf{Z}^k]$ is the updated state estimate conditioned on jth validated measurement having originated from target. The estimate using $\mathbf{A}(j)$ is

$$\tilde{\mathbf{x}}_i^{(j)}(k \mid k) = \hat{\mathbf{x}}_i(k \mid k-1) + \mathbf{K}_i(k)(\mathbf{z}_j(k) - \mathbf{H}\hat{\mathbf{x}}_i(k \mid k-1)), \tag{17}$$

where $\mathbf{K}_i(k)$ is the Kalman gain, and $\nu_j(k) = \mathbf{z}_j(k) - \mathbf{H}\hat{\mathbf{x}}_i(k \mid k-1)$ is the corresponding innovation. Given target originated measurement and predicted target state, innovation can be computed without ambiguity. But in (14) target state $\tilde{\mathbf{x}}_i(k \mid k)$ is computed with unknown target originated measurement. Using (17) and (14) the estimated target state is

$$\begin{aligned}\tilde{\mathbf{x}}_i^{(MMSE)}(k \mid k) &= \sum_j \tilde{\mathbf{x}}_i^{(j)}(k \mid k)\beta_j \\ &= \hat{\mathbf{x}}_i(k \mid k-1) + \mathbf{K}_i(k) \sum_{j=0:m_k} \nu_j(k)\beta_j(k).\end{aligned} \tag{18}$$

In (18) with index $j = 0$ the predicted measurement is used for updating the target state. Hence, the measurement prediction error is

$$\begin{aligned}\nu_0(k) &= \mathbf{z}_0(k) - \hat{\mathbf{z}}_i(k \mid k-1) \\ &= \hat{\mathbf{z}}_i(k \mid k-1) - \hat{\mathbf{z}}_i(k \mid k-1) = 0.\end{aligned} \tag{19}$$

Let $\tilde{\mathbf{z}}_i(k) = \sum_j \bar{\mathbf{z}}_j(k)\beta_j(k)$. The mean of the estimation error can be computed as

$$\begin{aligned} E(\boldsymbol{\epsilon}_{x,k}) &= E(\mathbf{x}_i(k) - \tilde{\mathbf{x}}_i^{(MMSE)}(k \mid k)) \\ &= E[\mathbf{x}_i(k) - \hat{\mathbf{x}}_i(k \mid k-1) - \mathbf{K}_i(k)\tilde{\mathbf{z}}_i(k)] \\ &= E[\boldsymbol{\epsilon}_{x_i,k-1}] - \mathbf{K}_i(k)E[\tilde{\mathbf{z}}_i(k)]. \end{aligned} \tag{20}$$

Therefore, if $E[\tilde{\mathbf{z}}_i(k)] = 0$ for every k and $E[\boldsymbol{\epsilon}_{x,k-1}] = 0$ then $E(\epsilon_{x,k}) = 0$ and the state estimate will be unbiased. PDA assumes only one measurement originated from target. But $\tilde{\mathbf{z}}_i(k)$ is computed using more than one measurement. On account of this measurement origin uncertainty exists in the computation of $\tilde{\mathbf{z}}_i(k)$ and the proposed approach attempts to model the measurement origin uncertainty by defining a random variable $\mathbf{q}_j(k)$. The proposed approach models the measurement origin uncertainty using $\mathbf{q}_j(k)$, so that $E[\tilde{\mathbf{z}}_i(k)] = 0$ and the target state will remain unbiased. If all measurements are modeled using (2), considering only the target originated case, then the measurement noise covariance is $\mathbf{R} = E[\mathbf{v}(k)\mathbf{v}(k)^T]$ as in PDA. But only one measurement among the validated measurement might have originated from target. Hence, under measurement origin uncertainty the measurement noise covariance can have two parts. The first part is a fixed known noise covariance $\mathbf{R}$ for the measurement originated from target and the second part denoted as $\boldsymbol{\Sigma}(k) = E[\mathbf{q}_j(k)\mathbf{q}_j(k)^T]$ is contributed by the uncertainty in the measurement origin. The uncertainty in measurement origin is computed using the spread of measurements. The random variable $\mathbf{q}_j(k)$ is used in the next subsection to define the spread of measurements. The modification of the measurement noise covariance affects the innovation covariance, Kalman gain and posterior error covariance as shown in the following sub-sections.

3. PROPOSED MEASUREMENT MODEL AND MODIFIED FILTER PARAMETERS

In PDA the target state estimate is obtained using combined innovation $\tilde{\mathbf{z}}_i(k)$ as given in (18). The combined innovation $\tilde{\mathbf{z}}_i(k)$ is obtained as

$$\begin{aligned} \tilde{\mathbf{z}}_i(k) &= \sum_j \bar{\mathbf{z}}_j(k)\beta_j(k) \\ &= \sum_{j=0:m_k} (\mathbf{z}_j(k) - \mathbf{H}\hat{\mathbf{x}}_i(k \mid k-1))\beta_j(k) \\ &= \sum_{j=0:m_k} (\mathbf{z}_j(k)\beta_j(k)) - \mathbf{H}\hat{\mathbf{x}}_i(k \mid k-1). \end{aligned} \tag{21}$$

Using (21) the target state estimate obtained by (18) can be rewritten as

$$\begin{aligned} \tilde{\mathbf{x}}_i^{(MMSE)}(k \mid k) &= \hat{\mathbf{x}}_i(k \mid k-1) \\ &+ \mathbf{K}_i(k)\left(\sum_{j=0:m_k} (\mathbf{z}_j(k)\beta_j(k)) - \mathbf{H}\hat{\mathbf{x}}_i(k \mid k-1)\right). \end{aligned} \tag{22}$$

In (22) the innovation is computed using the expectation of measurement $E[\mathbf{z}_j(k)] = \sum_{j=0:m_k} \mathbf{z}_j(k)\beta_j(k)$. Let the target originated measurement be denoted with index i, $\mathbf{z}_i(k)$. Therefore, posterior target state computed using (17) with index i is corresponding to the target originated measurement $\mathbf{z}_i(k)$. Comparing the expression for posterior target state in PDA (22) and with the posterior target state obtained with the target originated measurement, $\mathbf{z}_i(k)$ obtained with measurement index i in (17)

$$\begin{aligned} \tilde{\mathbf{z}}(k) &= \sum_{j=0:m_k} (\mathbf{z}_j(k)\beta_j(k)) = \mathbf{z}_i(k) \\ &= \mathbf{H}\mathbf{x}_i(k) + \mathbf{v}(k). \end{aligned} \tag{23}$$

If the measurement estimate $\tilde{\mathbf{z}}(k) = \mathbf{z}_i(k)$ then the PDA estimates computed using (22) is equal to the estimates obtained with known target originated measurement. Hence, $\tilde{\mathbf{z}}(k)$ is used as an estimate of $\mathbf{z}_i(k)$ and the error in using validated measurement for updating the state of target instead of the measurement that originated from the target is computed as, $\mathbf{q}_j(k) = \mathbf{z}_j(k) - \tilde{\mathbf{z}}(k)$. Substituting for $\tilde{\mathbf{z}}(k)$ from (23) gives

$$\mathbf{q}_j(k) = \mathbf{z}_j(k) - \sum_{j=0:m_k} \mathbf{z}_j(k)\beta_j(k). \tag{24}$$

Hence, using (23) the modified measurement model for the measurements obtained in the validation region is defined as

$$\begin{aligned} \mathbf{z}_j(k) &= \mathbf{z}_i(k) + \mathbf{q}_j(k) \\ &= \mathbf{H}\mathbf{x}_i(k) + \mathbf{v}(k) + \mathbf{q}_j(k), \end{aligned} \tag{25}$$

where, $\mathbf{v}(k) \sim \mathcal{N}(\mathbf{v}(k); 0, \mathbf{R})$ and $\mathbf{q}_j(k) \sim \mathcal{N}(\mathbf{q}_j(k); 0, \boldsymbol{\Sigma}(k))$. For the target originated measurement, substituting $j = i$ in (24)

$$\mathbf{q}_i(k) = \mathbf{z}_i(k) - \sum_{j=0:m_k} (\mathbf{z}_j(k)\beta_j(k)). \tag{26}$$

Using (23) in (26), gives $\mathbf{q}_i(k) = 0$, accordingly, the modified measurement model given in (25) becomes (2) for the target originated measurement. Under association hypothesis $\mathbf{A}(0)$ the target originated measurement may not be available inside the validation region and the predicted measurement $\hat{\mathbf{z}}_i(k \mid k-1) = \mathbf{H}\hat{\mathbf{x}}_i(k \mid k-1)$ is used for state update. Hence, under $\mathbf{A}(0)$ the target originated measurement $\mathbf{z}_i(k)$ is replaced with $\hat{\mathbf{z}}_i(k \mid k-1)$ and (25) becomes

$$\mathbf{z}_j(k) = \hat{\mathbf{z}}_i(k \mid k-1) + \mathbf{q}_j(k). \tag{27}$$

Using the identity $\sum_{j=0:m_k} \beta_j(k) = 1$, the expression for $\mathbf{q}_j(k)$ is rewritten as

$$\begin{aligned} \mathbf{q}_j(k) &= \mathbf{z}_j(k) - \sum_{j=0:m_k} \mathbf{z}_j(k)\beta_j(k) \\ &= \mathbf{z}_j(k) - \mathbf{H}\hat{\mathbf{x}}_i(k \mid k-1) \\ &\quad - \sum_{j=0:m_k} (\mathbf{z}_j(k) - \mathbf{H}\hat{\mathbf{x}}_i(k \mid k-1))\beta_j(k) \\ &= \nu_j(k) - E(\nu_j(k)). \end{aligned} \tag{28}$$

The expression for $\mathbf{q}_j(k)$ derived in (28) is used in the next subsection for computing $\mathbf{\Sigma}(k)$. The conventional PDA [12] assumes under hypothesis $\mathbf{A}(j)$ measurement $\mathbf{z}_j(k)$ is target originated. The association is carried out under the assumption that at the maximum only one measurement can be originated from target. If $\mathbf{z}_j(k)$ is target originated then β_j should be equal to one. The proposed model anticipates a non-ideal situation to identify the target originated measurement $\mathbf{z}_i(k)$ from the set of measurement $\mathbf{Z}(k) = \{\mathbf{z}_j(k)\}_{j=1:m_k}$, so has a provision to cater the uncertainties in case none of the $\beta(j)$ are equal to one. To satisfy $\mathbf{z}_i(k) = \sum_{j=0:m_k}(\mathbf{z}_j(k)\beta_j(k))$, the association probability $\beta_i(k)$ should be equal to one and $\beta_j(k) = 0$ for all $j \neq i$, because $\sum_{j=0:m_k}\beta_j(k) = 1$. If, $\max(\beta_j(k)) = 1$ then there is only one nonzero $\beta_j(k)$ value ($\beta_j(k) = p(\mathbf{A}(j) \mid \mathbf{Z}^k) = 1$) and there is no uncertainty in selecting $\mathbf{A}(j)$, so $\mathbf{\Sigma}(k) = 0$. But in practice, $\max(\beta_j(k)) < 1$ and this implies $\mathbf{\Sigma}(k) \neq 0$ and results in additional terms in measurement error covariance, innovation covariance and posterior target state error covariance. Conventional PDA modifies the posterior target state error covariance with an additional term corresponding to the measurement origin uncertainty. The proposed approach computes the additional additive terms and modifies the measurement error covariance and innovation covariance along with posterior target state error covariance. The additive term used for modifying the measurement error covariance is obtained as, $\mathbf{\Sigma}(k) = E[\mathbf{q}_j(k)\mathbf{q}_j^T(k) \mid \mathbf{Z}^k]$. An expression for computing is $\mathbf{\Sigma}(k)$ is derived in the next subsection.

3.1 Modified measurement error covariance

The modified measurement error covariance is computed using (25) as

$$\begin{aligned}\mathbf{R}^\theta(k) &= E[(\mathbf{z}_j(k) - \mathbf{H}\mathbf{x}_i(k))(\mathbf{z}_j(k) - \mathbf{H}\mathbf{x}_i(k))^T \mid \mathbf{Z}^k] \\ &= (E[\mathbf{v}(k)\mathbf{v}(k)^T] + E[\mathbf{q}_j(k)\mathbf{q}_j(k)^T \mid \mathbf{Z}^k]). \end{aligned} \quad (29)$$

In PDA the measurement likelihood is computed using the error covariance $\mathbf{R}(k)$ conditioned on the hypotheses that the given measurement alone is originated from the target. The modified measurement error covariance $\mathbf{R}^\theta(k)$ is the unconditional measurement error variance [31]. The unconditional measurement error covariance consists of an additional term. The additional error variance term corresponds to the error in using the validated measurement for updating the target state instead of measurement that originated from the target and this can be obtained using (24) as

$$\begin{aligned}&E[\mathbf{q}_j(k)\mathbf{q}_j(k)^T \mid \mathbf{Z}^k] \\ &\quad = E[(\mathbf{z}_j(k) - \tilde{\mathbf{z}}(k))(\mathbf{z}_j(k) - \tilde{\mathbf{z}}(k))^T \mid \mathbf{Z}^k].\end{aligned}$$

The first term of the measurement error covariance in (29) is computed as

$$E[\mathbf{v}(k)\mathbf{v}(k)^T] = \mathbf{R}. \quad (30)$$

The second term of the measurement error covariance can be obtained using (28) as

$$\begin{aligned}\mathbf{\Sigma}(k) &= E[\mathbf{q}_j(k)\mathbf{q}_j^T(k) \mid \mathbf{Z}^k] \\ &= E[(\nu_j(k) - E(\nu_j(k))) \\ &\quad (\nu_j(k) - E(\nu_j(k)))^T \mid \mathbf{Z}^k]. \end{aligned} \quad (31)$$

Using (30) and (31) in (29) the modified measurement error covariance can be computed as

$$\mathbf{R}^\theta(k) = \mathbf{R} + \mathbf{\Sigma}(k). \quad (32)$$

Assuming $\nu_j(k)$ are independent and identically distributed (i.i.d), as shown in [28], the expression for $\mathbf{\Sigma}(k)$ can be obtained from (31) as

$$\begin{aligned}\mathbf{\Sigma}(k) &= E[\nu_j(k)\nu_j(k)^T \mid \mathbf{Z}^k] \\ &\quad - E(\nu_j(k) \mid \mathbf{Z}^k)E(\nu_j(k) \mid \mathbf{Z}^k)^T \\ &= \sum_{j=0}^{m_k}\beta_j\nu_j(k)\nu_j(k)^T - \tilde{\mathbf{Z}}(k)\tilde{\mathbf{Z}}(k)^T, \end{aligned} \quad (33)$$

where $\tilde{\mathbf{Z}}(k) = E(\nu_j(k) \mid \mathbf{Z}^k)$. The expectation in (33) is over the measurement error $\nu_j(k) = \mathbf{z}_j(k) - \mathbf{H}\hat{\mathbf{x}}_i(k \mid k-1)$ and $\beta_j \propto p(\nu_j(k))$. The expression given in (33) is used in PDA filter for computing the posterior error covariance [12], [6]. For the case with $P_d = 1$ and $P_G = 1$ in (16), i.e., with $b = 0$ in (15) results in $\beta_0 = 0$ and the modified measurement error covariance is obtained as

$$\mathbf{R}^\theta(k) = \mathbf{R} + \mathbf{\Sigma}(k). \quad (34)$$

Hence, the modified measurement error covariance $\mathbf{R}^\theta(k)$ is adaptive with probability of detection P_d and also with measurement origin uncertainty.

3.2 Modified innovation covariance

The modified innovation covariance is computed by substituting $\mathbf{R}^\theta(k)$ instead of $\mathbf{R}$ in (11)

$$\mathbf{S}_i^\theta(k) = \mathbf{H}\mathbf{P}_i(k \mid k-1)\mathbf{H}^T + (1 - \beta_0)\mathbf{R} + \mathbf{\Sigma}(k). \quad (35)$$

For $\beta_0 = 0$ the modified innovation covariance is

$$\mathbf{S}_i^\theta(k) = \mathbf{S}_i(k) + \mathbf{\Sigma}(k). \quad (36)$$

where $\mathbf{S}_i(k)$ is the innovation covariance of target originated measurements and the term $\mathbf{\Sigma}(k)$ is used for computing the spread of innovation in [12]. The modified innovation covariance $\mathbf{S}_i^\theta(k)$ is used in (16) and (15) to find the data association probabilities in the proposed approach.

3.3 Posterior error covariance in PDA

The posterior covariance with measurement origin uncertainty can be obtained from Appendix D.3 of [12] as

$$\mathbf{P}_i(k \mid k) = E\left[(\mathbf{x}_i(k) - \tilde{\mathbf{x}}_i(k \mid k))(\mathbf{x}_i(k) - \tilde{\mathbf{x}}_i(k \mid k))^T \mid \mathbf{Z}^k\right], \quad (37)$$

$$\mathbf{P}_i(k \mid k) = \beta_0 \mathbf{P}_i(k \mid k-1) + (1-\beta_0)\mathbf{P}^*(k \mid k) + \mathbf{K}_i(k)\left(\sum_{j=0}^{m_k} \beta_j \bar{\mathbf{z}}_j \bar{\mathbf{z}}_j^T - \tilde{\mathbf{Z}}\tilde{\mathbf{Z}}^T\right)\mathbf{K}_i(k)^T, \tag{38}$$

where $\mathbf{P}^*(k \mid k)$ is the posterior covariance without measurement origin uncertainty, obtained in (10), and β_0 is the probability of updating the target state without having any valid measurement.

3.4 Modified filter gain

The objective in computing gain $\mathbf{K}$ in Kalman filter is to minimize the estimation error, by minimizing the trace of the posterior error covariance $\mathbf{P}(k \mid k)$. The target index i is dropped in this section for notational brevity. Substituting the expression for posterior covariance from (10) in (38) gives

$$\begin{aligned}\mathbf{P}(k \mid k) &= \beta_0 \mathbf{P}(k \mid k-1) \\ &\quad + (1-\beta_0)((\mathbf{I}-\mathbf{K}(k)\mathbf{H})\mathbf{P}(k \mid k-1) \\ &\quad \times (\mathbf{I}-\mathbf{K}(k)\mathbf{H})^T + \mathbf{K}(k)\mathbf{R}\mathbf{K}(k)^T) \\ &\quad + \mathbf{K}(k)\left(\sum_{j=0}^{m_k} \beta_j \nu_j \nu_j^T - \tilde{\mathbf{Z}}\tilde{\mathbf{Z}}^T\right)\mathbf{K}(k)^T. \end{aligned} \tag{39}$$

The gain $\mathbf{K}^\theta$ that minimizes the trace of $\mathbf{P}(k \mid k)$ (sum of the mean square errors in the estimates of all the elements of state vector) is obtained by computing the derivative with respect to $\mathbf{K}$ as

$$\begin{aligned}&\frac{d(\text{trace}\{\mathbf{P}(k \mid k)\})}{d\mathbf{K}} \\ &= 2(1-\beta_0)(\mathbf{I}-\mathbf{K}(k \mid k)\mathbf{H})\mathbf{P}(k \mid k-1)(-\mathbf{H})^T \\ &\quad + 2\mathbf{K}(k \mid k)((1-\beta_0)\mathbf{R} + \sum_{j=0}^{m_k} \beta_j \nu_j \nu_j^T - \tilde{\mathbf{Z}}\tilde{\mathbf{Z}}^T), \end{aligned} \tag{40}$$

and setting this equal to zero. The modified filter gain $\mathbf{K}^\theta$ is

$$\mathbf{K}^\theta(k) = \frac{(1-\beta_0)\mathbf{P}(k \mid k-1)\mathbf{H}^T}{(1-\beta_0)(\mathbf{H}\mathbf{P}(k \mid k-1)\mathbf{H}^T + \mathbf{R}) + \sum_{j=0}^{m_k} \beta_j \nu_j \nu_j^T - \tilde{\mathbf{Z}}\tilde{\mathbf{Z}}^T}. \tag{41}$$

The modified gain $\mathbf{K}^\theta$ obtained in (41) reduces to the standard Kalman gain

$$\mathbf{K}(k) = \frac{\mathbf{P}(k \mid k-1)\mathbf{H}^T}{\mathbf{H}\mathbf{P}(k \mid k-1)\mathbf{H}^T + \mathbf{R}} = \frac{\mathbf{P}(k \mid k-1)\mathbf{H}^T}{\mathbf{S}(k \mid k)} \tag{42}$$

under no measurement origin uncertainty. The quantity

$$\mathbf{\Sigma}(k) = \sum_{j=0}^{m_k} \beta_j \nu_j(k) \bar{\mathbf{z}}_j^T(k) - \tilde{\mathbf{Z}}(k)\tilde{\mathbf{Z}}^T(k),$$

will be zero if $\beta_j = 1$ for any j, ($\sum_{j=0:m_k} \beta_j = 1$). The target state conditioned on hypothesis $\mathbf{A}(j)$ denoted as $\tilde{\mathbf{x}}_i^{(j)}(k \mid k)$ is computed in (17) is conditioned on only one hypothesis $\mathbf{A}(j)$. Hence, the gain $\mathbf{K}(k)$ used in (17) is the standard Kalman gain. The modified filter gain is used in computing the posterior state error covariance because of the involvement of more than one association hypotheses. The posterior state error covariance computed using modified filter gain $\mathbf{K}^\theta(k)$ is referred as modified posterior state error covariance denoted by $\mathbf{P}^\theta(k \mid k)$.

The modified posterior state error covariance can be obtained by substituting $\mathbf{K}^\theta$ obtained by (41) in (39) as

$$\begin{aligned}\mathbf{P}^\theta(k \mid k) &= \beta_0 \mathbf{P}(k \mid k-1) + \\ &\quad (1-\beta_0)((\mathbf{I}-\mathbf{K}^\theta(k)\mathbf{H})\mathbf{P}(k \mid k-1)(\mathbf{I}-\mathbf{K}^\theta(k)\mathbf{H})^T \\ &\quad + \mathbf{K}^\theta(k)\mathbf{R}\mathbf{K}^\theta(k)^T) \\ &\quad + \mathbf{K}^\theta(k)\left(\sum_{j=0}^{m_k} \beta_j \nu_j \nu_j^T - \tilde{\mathbf{Z}}\tilde{\mathbf{Z}}^T\right)\mathbf{K}^\theta(k)^T. \end{aligned} \tag{43}$$

3.5 Iterative PDA (Iter-PDA)

The PDA approach uses Kalman filter (KF) framework and in KF the estimation process evolves with time and measurement update. The time update and measurement update steps involved in target tracking under MOU using PDA approach is shown in Fig. 2.

The modified innovation covariance is computed in the proposed approach using modified measurement error covariance $\mathbf{R}^\theta(k)$ instead of fixed measurement noise variance $\mathbf{R}$. The gain used for computing the covariance update in the measurement update step is also modified with the measurement error variance. The difference in the proposed approach compared to conventional PDA approach is shown with bold dotted arrows in Fig. 2. The main difference with conventional PDA is in computing the adaptive data association probabilities and modified filter gain as shown in Fig. 2. The proposed modifications in gain and association probabilities are obtained with dynamic measurement error variance $\mathbf{\Sigma}(k)$. The modified association probabilities are used for computing the combined target state estimate. The advantage of the proposed technique (Iter-PDA) is shown with Monte Carlo simulations in Sec. 5.

The modified innovation covariance $\mathbf{S}^\theta(k)$ computed using (35) can be written as

$$\begin{aligned}\mathbf{S}^\theta(k) &= \mathbf{H}\mathbf{P}(k \mid k-1)\mathbf{H}^T + (1-\beta_0)\mathbf{R} + \mathbf{\Sigma}(k), \\ &= \mathbf{H}\mathbf{P}(k \mid k-1)\mathbf{H}^T + \mathbf{R}^\theta(k). \end{aligned} \tag{44}$$

Therefore, by modifying the measurement model in Iter-PDA the measurement noise covariance is modified with an additive term $\mathbf{\Sigma}(k)$ corresponding to measurement origin uncertainty. The modified innovation

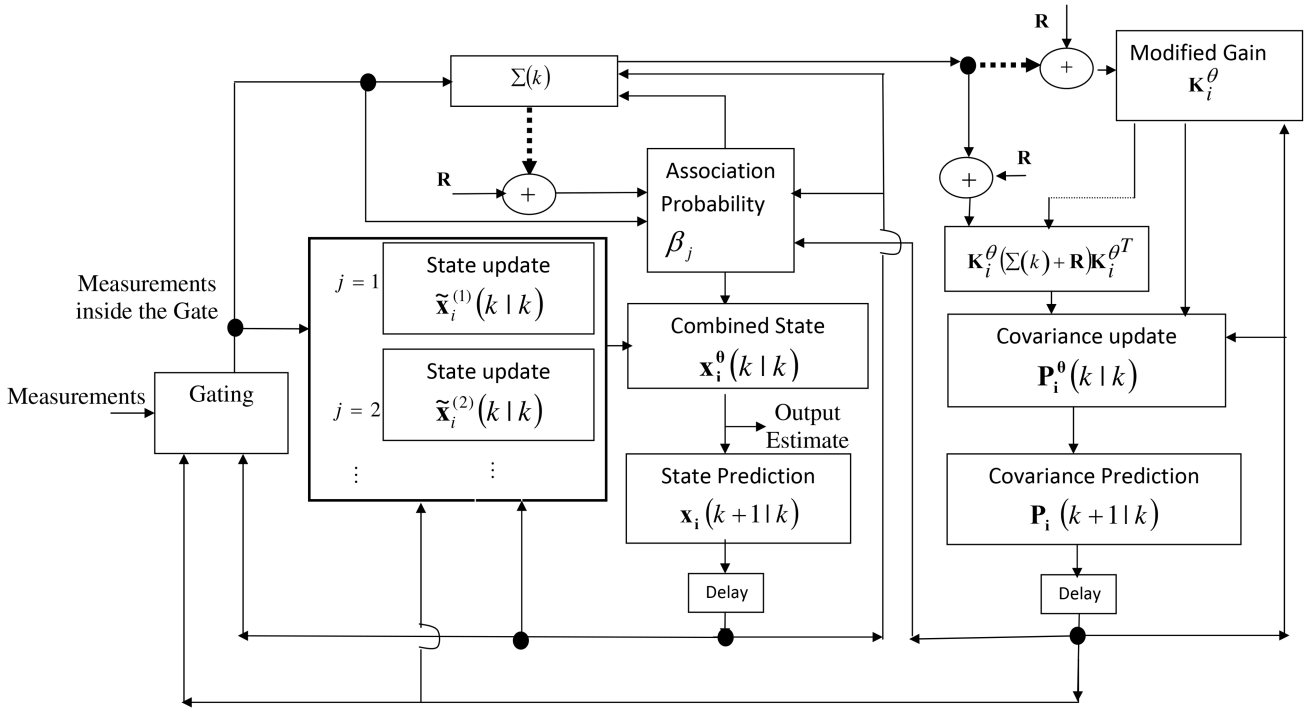

Fig. 2. A flow diagram for measurement update and time update in target tracking under MOU. Dotted thick arrows shown at two places indicate the proposed adaptations compared to PDA. With the proposed adaptation, fixed measurement noise covariance $\mathbf{R}$ becomes $\mathbf{R}^\theta(k) = \mathbf{R} + \mathbf{\Sigma}(k)$.

covariance and modified Kalman gain are due to the modified measurement noise covariance $\mathbf{R}^\theta(k)$. Using the modified innovation covariance $\mathbf{S}^\theta(k)$ and filter gain $\mathbf{K}^\theta(k)$ the PDA filter is modified and steps in the Iter-PDA algorithm are summarized as follows,

- Step 1: Compute posterior target state $\tilde{\mathbf{x}}_i^{(j)}(k \mid k)$ for $j = 0,\ldots,m_k$ with association hypothesis $\mathbf{A}(j)$, using (17).
- Step 2: Compute innovation covariance $\mathbf{S}^\theta(k)$ using (35). For first iteration, i.e., at $n = 1$, $\mathbf{\Sigma}(k)$ is unknown, as a result, $\mathbf{S}^\theta(k) = \mathbf{S}(k)$.
- Step 3: Compute filter gain $\mathbf{K}^\theta(k)$ using (41) and posterior covariance $\mathbf{P}^\theta(k \mid k)$ using (43).
- Step 4: Compute the association probabilities β_j using (15) with the modified innovation covariance $\mathbf{S}^\theta(k)$.
- Step 5: If β_j is different from the previous iteration go to Step 1. Otherwise iteration stops.
- Step 6: Target state in MMSE sense is estimated as $\mathbf{x}_i^\theta(k) = \sum_j \tilde{\mathbf{x}}_i^{(j)}(k \mid k)\beta_j$.
- Step 7: Compute the predicted state and covariance as

$$\mathbf{x}_i(k+1 \mid k) = \mathbf{F}\mathbf{x}_i^\theta(k \mid k), \tag{45}$$

$$\mathbf{P}_i(k+1 \mid k) = \mathbf{F}\mathbf{P}_i^\theta(k \mid k)\mathbf{F}^T + \mathbf{Q}. \tag{46}$$

The difference between PDA and the proposed Iter-PDA is in the computation of the modified measurement noise covariance $\mathbf{R}^\theta(k)$ and the modified innovation covariance $\mathbf{S}^\theta(k)$. With this modification, $\mathbf{R}^\theta(k) \geq \mathbf{R}$ and $\mathbf{S}^\theta(k) \geq \mathbf{S}(k)$ because $\mathbf{\Sigma}(k)$ is positive semi-definite, as shown in Appendix D.3 of [12]. The additive term $\mathbf{\Sigma}(k)$ becomes zero with $\beta_j = 1$. The instantaneous adaptability of Iter-PDA is achieved by modifying the filter parameters $\mathbf{R}^\theta(k)$, $\mathbf{S}^\theta(k)$, $\mathbf{K}^\theta(k)$ and $\mathbf{P}^\theta(k \mid k)$ with MOU. In the absence of MOU these parameters are the standard Kalman filter parameters. In the case of conventional PDA given in [5], [6], [12], [13] the posterior error covariance $\mathbf{P}(k \mid k)$ is the only term that changes with MOU. Therefore, in conventional PDA the effect of MOU at time instant k will appear on filter parameters ($\mathbf{S}(k+1)$, $\mathbf{K}(k+1)$) at the subsequent time instant $k+1$.

The term $\mathbf{\Sigma}(k)$ in modified innovation covariance $\mathbf{S}^\theta(k)$ is a function of β_j, $j = 0,\ldots,m_k$ as shown in (33). But, the proposed approach computes β_j, $j = 0,\ldots,m_k$ using $\mathbf{S}^\theta(k)$ in (16). Hence, the process of computing $\mathbf{S}^\theta$ becomes iterative and the iteration process stops when the nth iterated $\beta_j^{(n)}$, $j = 1,\ldots,m_k$ does not change, i.e.

$$\sum_j |\beta_j^{(n)} - \beta_j^{(n-1)}| < \upsilon, \tag{47}$$

where υ is a sufficiently small, pre-defined quantity. The iteration process increases the measurement likelihood as shown in Appendix B. Because of the iterative computation of association probabilities the proposed approach is referred here as Iter-PDA. The Iter-JPDA developed in [19] computes the association probabili-

ties using the iteratively computed maximum a posterior estimates. The proposed approach here computes the association probabilities and innovation covariance by solving (33, 35) and (15, 16) iteratively.

4. CRLB WITH MOU USING MONTE CARLO AVERAGING TECHNIQUE

In target tracking with MOU the tracking performance can be evaluated by comparing how close the mean square error (MSE) is to the theoretical lower bound of the estimation error. This bound obtained as Cramér-Rao lower bound (CRLB) is shown to be the equivalent to the error covariance matrix [23] of the Kalman filter for the linear Gaussian case without MOU. The CRLB with MOU will also provide a mechanism to compare the performance of the proposed approach and PDA approach. In this section a recursive form of CRLB with measurement origin uncertainty is computed for the linear Gaussian case using the measurement model proposed in Sec.3. The difficulty in obtaining the CRLB with MOU is in the computation of information reduction factor (IRF). The approach given in [9], [24] requires computationally intensive numerical integration for the computation of IRF. The other alternative is to use tabulated values given in [27], [30] for a fixed filter parameter case. The approach developed in this section depend on Monte Carlo runs and is applicable to any filter parameters and clutter density.

Let $\tilde{\mathbf{x}}_i(k \mid k)$ be an unbiased estimate of $\mathbf{x}_i(k)$. The error covariance of $\tilde{\mathbf{x}}_i(k \mid k)$ denoted as $\mathbf{P}_i(k \mid k)$ has a lower bound referred to as the CRLB on the estimation error and is expressed as [23]

$$\begin{aligned}\mathbf{P}_i(k \mid k) &= E[(\tilde{\mathbf{x}}_i(k \mid k) - \mathbf{x}_i(k))(\tilde{\mathbf{x}}_i(k \mid k) - \mathbf{x}_i(k))^T] \\ &\geq \mathbf{J}^{-1}(k), \end{aligned} \tag{48}$$

where the lower bound $\mathbf{J}(k)$ is denoted without target index for notational brevity and can be obtained as

$$\begin{aligned}\mathbf{J}(k) &= E[[\nabla_{\mathbf{x}_i(k)} \log p(\mathbf{x}_i(k), \mathbf{z}_j(k))] \\ &\qquad [\nabla_{\mathbf{x}_i(k)} \log p(\mathbf{x}_i(k), \mathbf{z}_j(k))]^T] \\ &= -E[\nabla_{\mathbf{x}_i(k)} [\nabla_{\mathbf{x}_i(k)} \log p(\mathbf{x}_i(k), \mathbf{z}_j(k))]^T]. \end{aligned} \tag{49}$$

An unbiased state estimator with covariance matrix equal to CRLB (holding equality in (48)) is statistically efficient [22], [23]. A recursive form of information matrix $\mathbf{J}(k)$ can be obtained as in [34]

$$\begin{aligned}\mathbf{J}(k+1) &= D^{22}(k) \\ &\quad - D^{21}(k)(\mathbf{J}(k) + D^{11}(k))^{-1} D^{12}(k), \quad (k > 0), \end{aligned} \tag{50}$$

where the terms $D^{i_1 i_2}(k)$ can be computed as

$$\begin{aligned} D^{11}(k) &= -E\{\nabla_{\mathbf{x}_i(k)} [\nabla_{\mathbf{x}_i(k)} \log p(\mathbf{x}_i(k+1) \mid \mathbf{x}_i(k))]^T\} \\ D^{21}(k) &= -E\{\nabla_{\mathbf{x}_i(k)} [\nabla_{\mathbf{x}_i(k+1)} \log p(\mathbf{x}_i(k+1) \mid \mathbf{x}_i(k))]^T\} \\ D^{12}(k) &= -E\{\nabla_{\mathbf{x}_i(k+1)} [\nabla_{\mathbf{x}_i(k)} \log p(\mathbf{x}_i(k+1) \mid \mathbf{x}_i(k))]^T\} \\ D^{22}(k) &= -E\{\nabla_{\mathbf{x}_i(k+1)} [\nabla_{\mathbf{x}_i(k+1)} \log p(\mathbf{x}_i(k+1) \mid \mathbf{x}_i(k))]^T\} \\ &\quad - E\{\nabla_{\mathbf{x}_i(k+1)} [\nabla_{\mathbf{x}_i(k+1)} \log p(\mathbf{z}_j(k+1) \mid \mathbf{x}_i(k+1))]^T\}. \end{aligned} \tag{51}$$

In (51) $\nabla_{\mathbf{x}_i(k)}$ is the first-order partial derivative operator with respect to $\mathbf{x}_i(k)$. The expectation operator is defined as [23]

$$\begin{aligned} &- E\{\nabla_{\mathbf{x}_i(k)} [\nabla_{\mathbf{x}_i(k)} \log p(.)]^T\} \\ &\qquad = E\{[\nabla_{\mathbf{x}_i(k)} \log p(.)][\nabla_{\mathbf{x}_i(k)} \log p(.)]^T\}, \end{aligned} \tag{52}$$

and $D^{12}(k) = [D^{21}(k)]^T$. Using the state evolution (1) and the modified measurement error covariance (34), the terms inside the expectation of (51) can be evaluated as

$$\begin{aligned} &\nabla_{\mathbf{x}_i(k)} \log p(\mathbf{x}_i(k+1) \mid \mathbf{x}(k)) \\ &\qquad = \nabla_{\mathbf{x}_i(k)} - \tfrac{1}{2}[[\mathbf{x}_i(k+1) - \mathbf{F}\mathbf{x}_i(k)]^T \mathbf{Q}^{-1}(k) \\ &\qquad [\mathbf{x}_i(k+1) - \mathbf{F}\mathbf{x}_i(k)]] \\ &\qquad = \mathbf{F}^T \mathbf{Q}^{-1}(k)[\mathbf{x}_i(k+1) - \mathbf{F}\mathbf{x}_i(k)]. \end{aligned} \tag{53}$$

Similarly

$$\begin{aligned} &\nabla_{\mathbf{x}_i(k+1)} \log p(\mathbf{z}_j(k+1) \mid \mathbf{x}_i(k+1)) \\ &\qquad = \nabla_{\mathbf{x}_i(k+1)} - \tfrac{1}{2}[[\mathbf{z}_j(k+1) - \mathbf{H}\mathbf{x}_i(k+1)]^T \\ &\qquad \times (\mathbf{R}^\theta(k+1))^{-1} [\mathbf{z}_j(k+1) - \mathbf{H}\mathbf{x}_i(k+1)]] \\ &\qquad = \mathbf{H}^T (\mathbf{R}^\theta(k+1))^{-1} [\mathbf{z}_j(k+1) - \mathbf{H}\mathbf{x}_i(k+1)], \end{aligned} \tag{54}$$

where $\mathbf{R}^\theta(k+1)$ is the modified measurement error variance and obtained in (34) as

$$\mathbf{R}^\theta(k+1) = \mathbf{R} + \Sigma(k+1). \tag{55}$$

The matrices defined in (51) are computed using (54) and (55) as follows

$$\begin{aligned} D^{11}(k) &= E\{\nabla_{\mathbf{x}(k)} [\nabla_{\mathbf{x}(k)} \log p(\mathbf{x}(k+1) \mid \mathbf{x}(k))]^T\} \\ &\qquad = E\{\mathbf{F}^T \mathbf{Q}^{-1}(k) \mathbf{F}\} = \mathbf{F}^T \mathbf{Q}^{-1}(k) \mathbf{F}, \\ D^{12}(k) &= -\mathbf{F}^T \mathbf{Q}^{-1}(k), \\ D^{22}(k) &= \mathbf{Q}^{-1}(k) + E\{\mathbf{H}^T (\mathbf{R}^\theta(k+1))^{-1} \mathbf{H}\} \\ &\qquad = \mathbf{Q}^{-1}(k) + \mathbf{H}^T E\{(\mathbf{R}^\theta(k+1))^{-1}\} \mathbf{H}. \end{aligned} \tag{56}$$

The only term in the computation of $\mathbf{J}(k+1)$ that depends on measurements is $D^{22}(k)$. Using (56) in (50)

the recursive form of $\mathbf{J}(k+1)$ can be rewritten as

$$\mathbf{J}(k+1) = \mathbf{Q}^{-1}(k) + \mathbf{H}^T E\{(\mathbf{R}^{\theta}(k+1))^{-1}\}\mathbf{H} - \mathbf{Q}^{-1}(k)\mathbf{F}(\mathbf{J}(k) + \mathbf{F}^T\mathbf{Q}^{-1}(k)\mathbf{F})^{-1}\mathbf{F}^T\mathbf{Q}^{-1}(k). \quad (57)$$

The difficulty in computing $\mathbf{J}(k+1)$ using (57) is the presence of the expectation operator. We use a Monte Carlo approximation of $\mathbf{J}(k+1)$ as suggested by [23]. The term $E\{(\mathbf{R}^{\theta}(k+1))^{-1}\}$ can be obtained, from Appendix A, as

$$E\{(\mathbf{R}^{\theta}(k+1))^{-1}\} = E\{(\mathbf{R} + \mathbf{\Sigma}(k+1))^{-1}\} = q_2\mathbf{R}^{-1}, \text{ where } q_2 < 1. \quad (58)$$

Here q_2 is the scalar information reduction factor (IRF). Substituting (58) in (57), the CRLB with MOU can be obtained as

$$\mathbf{J}(k+1) = \mathbf{Q}^{-1}(k) + \mathbf{H}^T q_2\mathbf{R}^{-1}(k+1)\mathbf{H} - \mathbf{Q}^{-1}(k)\mathbf{F}(\mathbf{J}(k) + \mathbf{F}^T\mathbf{Q}^{-1}(k)\mathbf{F})^{-1}\mathbf{F}^T\mathbf{Q}^{-1}(k). \quad (59)$$

The CRLB for the target state $\mathbf{x}_i(k)$ can be obtained from the inverse of the information matrix $\mathbf{J}(k)$ as [22], [23]

$$\text{CRLB}(\mathbf{x}_i(k)) = \mathbf{J}^{-1}(k). \quad (60)$$

A deterministic expression for the CRLB consisting of higher order integrals for evaluating the expectation operation in (58) over all possible validated measurements can be obtained as shown in [27]. One way to avoid the computation of higher order integral is to use the tabulated values for IRF. The tabulated values of IRF given in [27], [30] are for $q = 1$ and $\mathbf{R} = \mathbf{I}$, but for different q and $\mathbf{R}$ the IRF values will be different. The values of IRF are shown to depend on q, $\mathbf{R}$, λ and P_d [27], [28]. But, in the simulations carried out in this paper with high clutter density it is observed that the IRF also depends on the time index k (Fig. 10[a] shows variation of IRF with k). The simulation results indicate the information reduction decreases when a filter attains steady state. The RMS positional error provided in the next section are computed using Monte Carlo simulations. Therefore, the CRLB is obtained as an auxiliary result of the simulations. In fact the tracker performance evaluation based on Monte Carlo simulation does not require additional MC runs for the computation of CRLB.

5. SIMULATIONS

To compare the proposed approach with PDA, an example scenario having state vector $\mathbf{x}^T = [x\ \dot{x}; y\ \dot{y}]^T$ and initial condition $\mathbf{x}^T = [200\,0; 10000; -15]^T$ is considered [12]. The system evolves according to

$$\mathbf{x}(k+1) = \mathbf{F}\mathbf{x}(k) + \mathbf{\Gamma}\mathbf{w}(k), \quad (61)$$

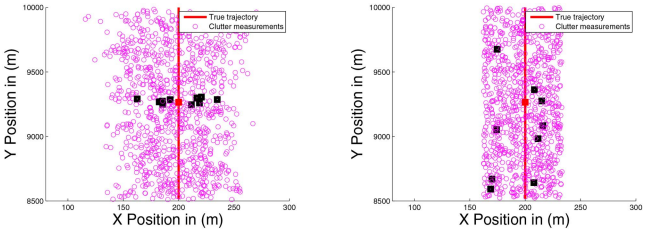

Fig. 3. Scenario in X-Y plane. Clutter measurements obtained from cumulative time instants (k = 1 to 100) are plotted with magenta circles. Clutter measurements at $k = 50$ are shown with bold black squares. True position at $k = 50$ is shown with red bold square. (a) Case (i): Clutter measurements are uniformly distributed in a square centered around the correct measurement (b) Case (i): Clutter measurements are uniformly distributed in surveillance region.

where $\mathbf{\Gamma} = \begin{bmatrix} T^2/2 & 0 \\ T & 0 \\ 0 & T^2/2 \\ 0 & T \end{bmatrix}$ and the time interval $T =$ 1 s. The process noise covariance and state transition matrices are

$$\mathbf{Q} = \begin{bmatrix} \mathbf{Q}_1 & \mathbf{0} \\ \mathbf{0} & \mathbf{Q}_1 \end{bmatrix} q, \quad \mathbf{F} = \begin{bmatrix} \mathbf{F}_1 & \mathbf{0} \\ \mathbf{0} & \mathbf{F}_1 \end{bmatrix}, \quad (62)$$

where

$$\mathbf{Q}_1 = \begin{bmatrix} \frac{T^4}{4} & \frac{T^3}{2} \\ \frac{T^3}{2} & T^2 \end{bmatrix}, \quad \mathbf{F}_1 = \begin{bmatrix} T & 1 \\ 0 & 1 \end{bmatrix}. \quad (63)$$

The process noise is a zero mean white sequence with variance, $E[\mathbf{w}(k)^2] = q^2$. Measurement noise is a zero mean white sequence with variance

$$\mathbf{R} = \begin{bmatrix} 200 & 0 \\ 0 & 200 \end{bmatrix}.$$

The state error covariance is initialized according to the two-point differencing method [32], [35]. The measurements are assumed to be obtained from target as well as from clutter. The clutter measurements are generated in two ways. In case (i), the clutter points are uniformly distributed in a square having area $A = 10\pi\gamma|\mathbf{S}(k)|^{1/2}$ and centered around the correct measurement (known in simulation) [12]. In case (ii), clutter measurements are distributed uniformly in a rectangular area covering the surveillance region. The surveillance region is defined by minimum and maximum X-Y coordinates of the trajectory. The scenario is shown in X-Y plane in Fig. 3 for $q = 0$. Compared to the case (i) shown in Fig. 3(a), the number of clutter measurements will be lower inside the gate for case (i) shown in Fig. 3(b), because of the spread of measurements across the surveillance region. Clutter measurements at $k = 50$ is shown in Fig. 3 to demonstrate the difference in spread of measurements.

The advantage of Iter-PDA will be significantly visible with more clutter points inside the gate. Therefore,

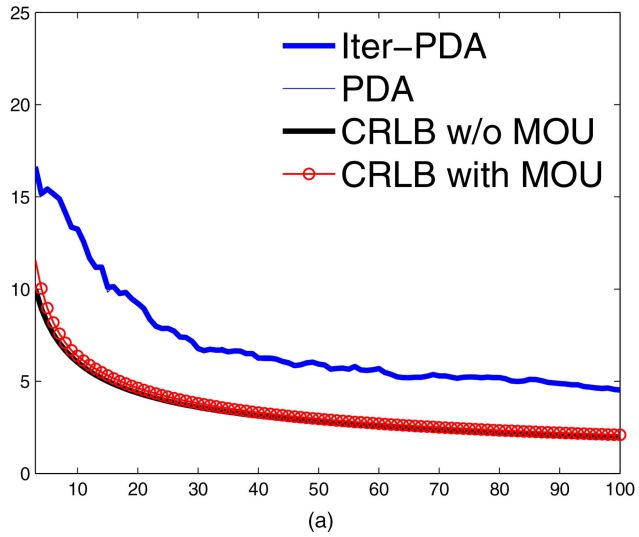

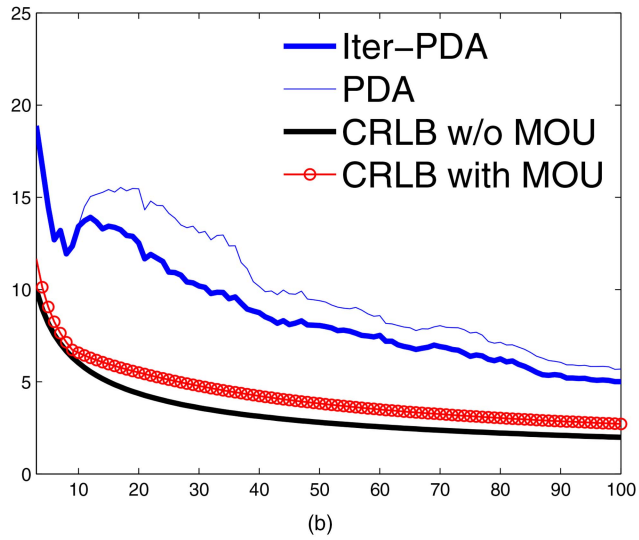

Fig. 4. RMS positional error (in m) versus time index k, with conventional and the proposed approach with $\gamma = 1$ and $q = 0$ for varying clutter densities (a) $\lambda = 1e^{-4}$. (b) $\lambda = 1e^{-3}$.

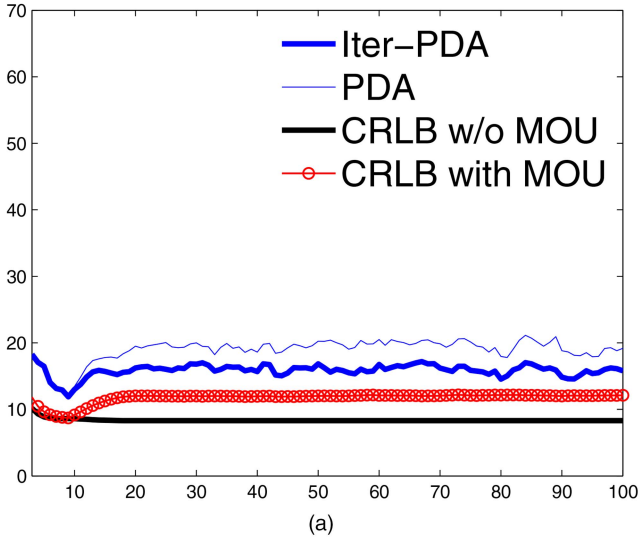

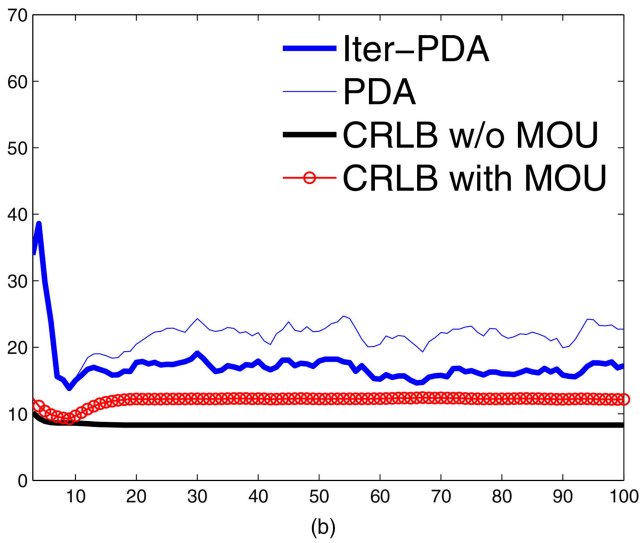

Fig. 5. RMS positional error (in m) versus time index k, with conventional and the proposed approach with $\gamma = 1$, $\bar{m}_k = 10$ and $q = 1$ for varying probability of detection (a) $P_d = 1$. (b) $P_d = 0.9$.

the simulations results with case (i) are provided in Fig. 4 to Fig. 6. The results with case (ii) is provided in Fig. 7. The parameter γ controlling the gate area is defined in Section 2. The average number of clutter points $\bar{m}_k = \lambda A$ per measurement frame is assumed to be Poisson distributed, where λ is the clutter density. The average number of iterations in Iter-PDA was five. In this section the performance of the Iter-PDA approach and PDA are compared to the CRLB. The CRLB and the information reduction factor (IRF) with MOU are computed for various filter parameters and clutter densities. The IRF variation pattern with λ and time index k were analyzed using Monte Carlo simulations. The consistency of Iter-PDA filter is also checked and compared with that of PDA under various P_d, λ and q.

5.1 Estimation performance

The root mean square (RMS) positional error for 100 Monte Carlo (MC) runs with $q = 0$ is plotted in Fig. 4(a), Fig. 4(b) with $\gamma = 1$, $\lambda = 1e^{-4}$ and $\lambda = 1e^{-3}$, respectively. The clutter measurements are introduced at time index $k = 10$. The clutter measurements are are uniformly distributed in a square centered around the correct measurement as described in case (i). The number of clutter measurements are obtained in parametric form and non-parametric form.

Parametric form: The PDA and the proposed Iter-PDA approach computes β_j in parametric form using the known λ values in (15) and (16). As shown in Fig. 4(a) the RMS positional error for the proposed approach (Iter-PDA) and PDA are not significantly different with $\lambda = 1e^{-4}$. But, with $\lambda = 1e^{-3}$ estimation accuracy is improved with Iter-PDA.

Non-parametric form: For simulations carried out with $q = 1$ a higher process error covariance is obtained and this lead to higher $\mathbf{S}(k)$, large gate area A and subsequently to large number of clutter measurements. Hence, instead of keeping λ fixed, the simulations are

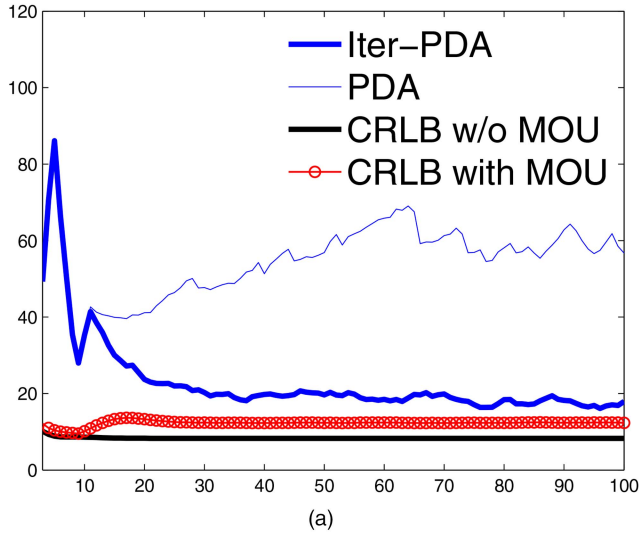

Fig. 6. RMS positional error (in m) versus time index k, with conventional and the proposed approach with $\gamma = 1$, for varying clutter densities, process noise and probability of detection (a) $\bar{m}_k = 10$, $q = 1$ and $P_d = 0.7$. (b) $\lambda = 1e^{-2}$, $q = 0$ and $P_d = 1$.

done with fixed $\bar{m}_k = A\lambda$ for $q = 1$ case. Similarly for $P_d < 1$ the simulations are done with fixed $\bar{m}_k = A\lambda$. The PDA and the proposed Iter-PDA approach computes β_j in non-parametric form using the computed λ values ($\lambda = \bar{m}/A$) in (15) and (16).

The RMS positional error with $\bar{m}_k = 10$ and with $q = 1$ and $P_d = 1$, $P_d = 0.9$ are provided in Fig. 5(a) and Fig. 5(b), respectively. Comparing Fig. 4 and Fig. 5 the increase in the CRLB with MOU is significant for $q = 1$ compared to $q = 0$. The RMS positional error in PDA increases more compared to Iter-PDA with $P_d = 0.9$. The RMS positional errors for 100 MC runs are provided in Fig. 6(a), for average number of clutter $\bar{m}_k = 10$ and $q = 1$ with $P_d = 0.7$.

The RMS error in PDA increases with decrease of P_d as shown in Fig. 5 and Fig. 6(a). The RMS positional error with higher clutter density compared to the results given in Fig. 4, i.e., $\lambda = 1e^{-2}$, $q = 0$ and $P_d = 1$ is provided in Fig. 6(b). Compared to conventional PDA, the proposed approach gives significantly better estimation accuracy with higher amount of clutter as depicted in Fig. 6(b). The estimation accuracy with Iter-PDA is always better than PDA with $\gamma = 1$. The sudden increase in error at time instant $k = 10$ onwards in Fig. 4, Fig. 5 and Fig. 6 is due to the introduction of clutter. The increase in position and velocity errors in Iter-PDA because of the introduction of clutter is low compared to PDA. But with $\gamma = 2$, $\gamma = 3$ and $\gamma = 4$ the advantage of Iter-PDA will be visible only with $\bar{m}_k = 50$ and $\bar{m}_k = 100$. Higher value of γ indicates measurement sparseness and so Iter-PDA is unable to extract additional information from measurements. In the proposed approach $\mathbf{q}_j(k)$ is approximated as a Gaussian random variable with mean zero and variance $\mathbf{\Sigma}_k$. With higher values of γ the innovation $\nu_j(k)$ and $\mathbf{q}_j(k)$ are widely spread around the predicted position. Hence, the approximation $\mathbf{q}_j(k) \sim \mathcal{N}(\mathbf{q}_j(k); 0, \mathbf{\Sigma}(k))$ may not be valid with higher values of γ. Hence, the proposed iterations are done only if the average likelihood is above a threshold, i.e., $(1/\bar{m}_k)\sum_{j=m_k} p(z_j(k) \mid \mathbf{A}(j), \mathbf{Z}^{k-1}) > \delta$. In this paper $\delta = 0.1$ has been used for the simulations.

The simulation results for the case (ii), with a uniform clutter pattern, are provided in Fig. 7. Here, the uniform clutter pattern is generated in an area A covering the entire surveillance region. With $\lambda = 1e^{-3}$ and $P_d = 1$ performance of PDA and Iter-PDA are similar. The RMS error obtained without MOU, i.e., by using the correct measurement in the standard Kalman filter based estimation has been carried out. The estimation with correct measurement is carried out to compare the performance of PDA and Iter-PDA against an ideal data association approach. In the absence of actual measurements, i.e., with $P_d < 1$, the predicted measurement is used for state update. With $P_d = 0.7$ the RMS error in position has been improved with Iter-PDA as shown in Fig. 7(a). The RMS positional error has been shown in Fig. 7(b) with $q = 0.1$. The RMS error without MOU shows slight increase at $k = 10$ due to the introduction of $P_d = 0.7$ from 10th instant. In both cases, Iter-PDA performs better than PDA and the estimation without MOU gives the best result as expected.

5.2 Information reduction factor (IRF) with MOU

The value of information reduction factor (IRF) q_2 for various cases of q and $\mathbf{R}$ are computed using the simulation scenario described in the previous sub-section with the clutter measurements generated using the case (i). The scalar and matrix IRF obtained with different pattern of measurement noise covariance $\mathbf{R}$ is summarized in [27]. The objective of this section is to check the scalar nature of IRF q_2 for diagonal measurement noise covariance. The case of measurement noise covariance $\mathbf{R}$ being a scalar multiple of identity matrix is considered here and the IRF $q_2(k)$ is shown to be a

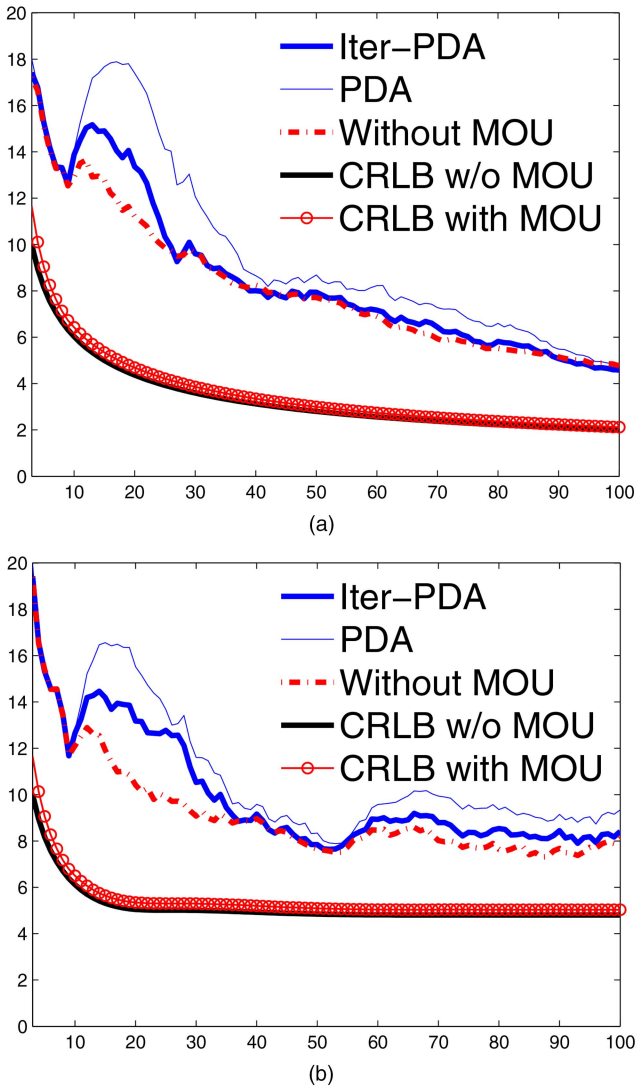

Fig. 7. RMS positional error (in m) versus time index k, with conventional and the proposed approach with $\gamma = 1$, $P_d = 0.7$ for varying process noise. Clutter is generated in an area having coordinates covering the entire surveillance region (a) $q = 0$ (b) $q = 0.1$.

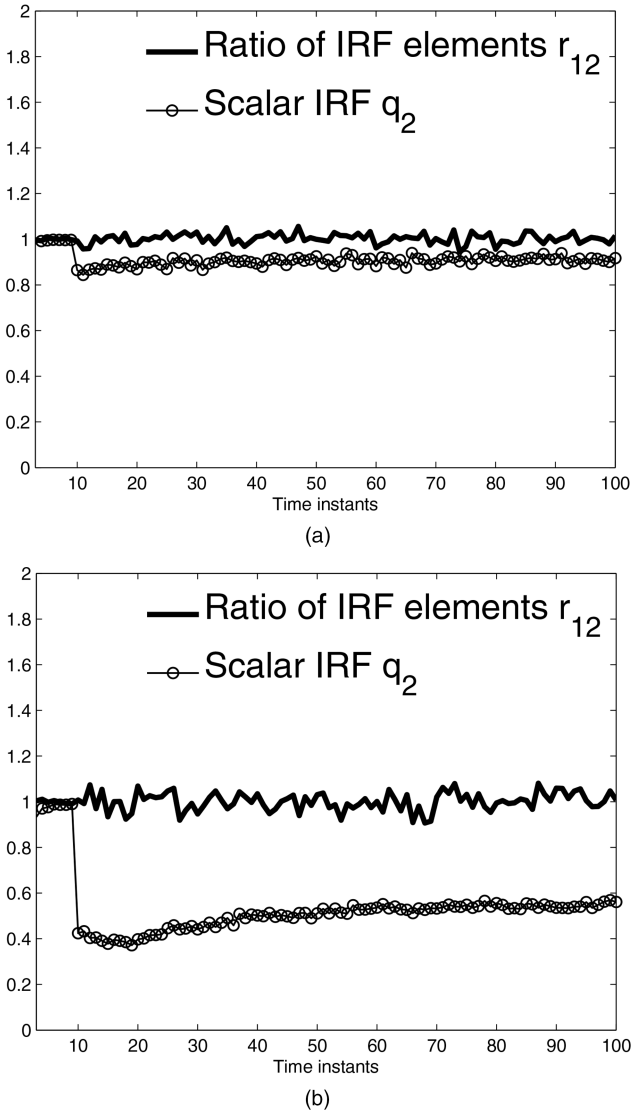

Fig. 8. The ratio of diagonal elements $r_{12}(k) = d_{11(k)}/d_{22}(k)$ and $q_2(k)$ versus time index k with conventional and with the proposed approach with $\gamma = 1$ for varying clutter densities. (a) $\lambda = 1e^{-4}$. (b) $\lambda = 1e^{-3}$.

scalar for all k. The IRF $q_2(k)$ will be a scalar if ratio d_{ii} of all the diagonal elements of $\mathbf{R}^{\theta(k)^{-1}}$ and $\mathbf{R}^{-1}$ are equal. The ratio d_{ii} is obtained as $d_{ii}(k) = \dfrac{\mathbf{R}^{\theta}_{ii}(k)^{-1}}{\mathbf{R}^{-1}_{ii}(k)}$ and for two-dimensional case $r_{12}(k) = \dfrac{d_{11(k)}}{d_{22(k)}}$. For $r_{12}(k) = 1$, $q_2(k) = d_{11}(k) = d_{22}(k)$. The IRF $q_2(k)$ and the ratio $r_{12}(k)$ are plotted in Fig. 8(a) and Fig. 8(b) with $\lambda = 1e^{-4}$ and $\lambda = 1e^{-3}$, for $\gamma = 1$, $\mathbf{R} = \begin{bmatrix} 200 & 0 \\ 0 & 200 \end{bmatrix}$ and $q = 0$. In Fig. 8, $r_{12} = 1$ indicates the elements of $\mathbf{R}^{\theta}(k)^{-1}$ are obtained by multiplying the elements of $\mathbf{R}(k)^{-1}$ with a scalar. The scalar $q_2(k)$ is less than one as shown in Fig. 8. In a clutter free zone $q_2(k) = 1$ and there is no information reduction. The value of $q_2(k)$ reduces, with increase in clutter density $\lambda = 1e^{-3}$ as shown in Fig. 8(b).

The variation of q_2 with low P_d and high clutter are analyzed in Fig. 9(a) and Fig. 9(b), respectively. The value of $q_2(k)$ and $r_{12}(k)$ are computed with $\bar{m}_k = 10$, $q = 1$, $P_d = 0.7$ and depicted in Fig. 9(a). Similarly $q_2(k)$ and $r_{12}(k)$ for $\lambda = 1e^{-2}$, $q = 0$, and $P_d = 1$ is provided in Fig. 9(b). In all the cases considered here for simulations, the ratio $r_{12}(k) = 1$ indicates that $q_2(k)$ is scalar and verifies the results obtained in [9], [24]. For $\lambda = 1e^{-3}$ and $\lambda = 1e^{-2}$ the scalar IRF q_2 is not a constant with time k. The variations are zoomed and shown in Fig. 10(a). In the initial time instants q_2 is low and as filter stabilizes q_2 increases. This suggests that the information loss due to clutter is less as the filter reaches steady state. The variations in trace of posterior state error covariance is plotted in Fig. 10(b). The trace increases rapidly with the introduction of clutter at $k = 10$ in PDA. In Iter-PDA the raise is nominal and this is due

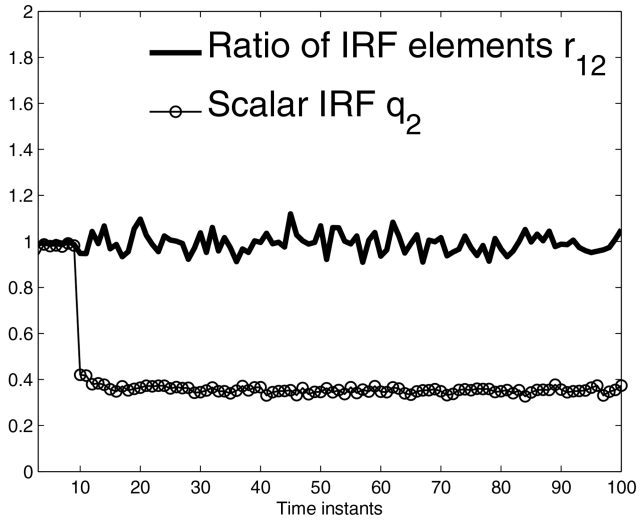

(a)

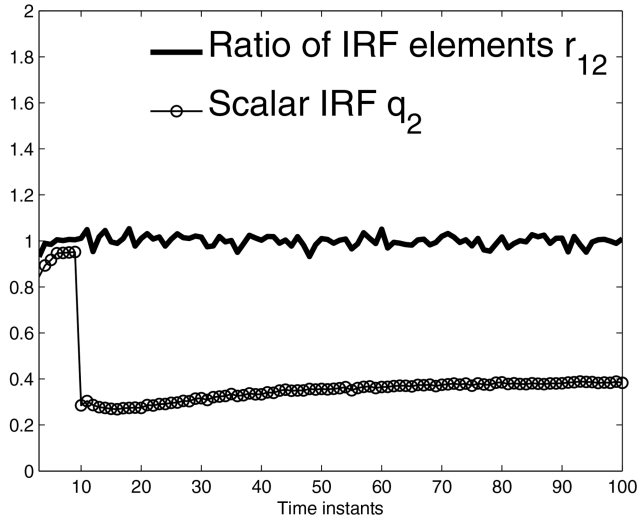

(b)

Fig. 9. The ratio of diagonal elements $r_{12}(k) = d_{11}(k)/d_{22}(k)$ and $q_2(k)$ versus time index k, with conventional and proposed approach with $\gamma = 1$ for varying clutter densities, process noise and probability of detection. (a) $\bar{m}_k = 10$, $q = 1$, $P_d = 0.7$ (b) $\lambda = 1e^{-2}$, $q = 0$, $P_d = 1$.

to the adaptability of Iter-PDA to adjust with clutter by modifying the innovation error covariance.

5.3 Consistency of Iter-PDA

The consistency of the proposed Iter-PDA filter is verified using the following three criteria [12], [35]:

1) Normalized state estimation error square (NEES) should be within an acceptable limit.
2) Normalized innovation square (NIS) should be within an acceptable limit.
3) Innovation should be acceptable as white.

The computation of acceptable limit for the above three criteria are given in [12], [35]. In this section numerical values of NEES, NIS and whiteness of innovation are checked with filter consistency acceptance limits. In [12] PDA filter consistency has been checked

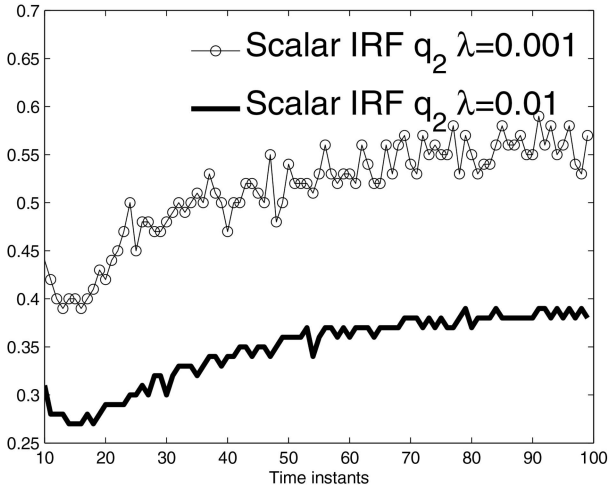

(a)

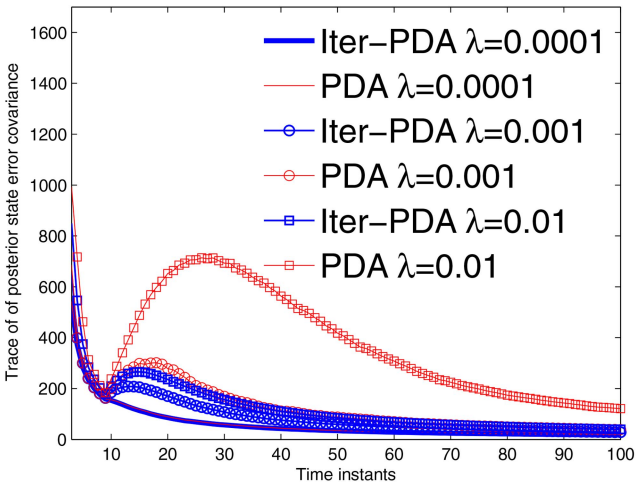

(b)

Fig. 10. (a) Zoomed-in section of q_2 for $\lambda = 1e^{-3}$ and $\lambda = 1e^{-2}$. (b) Trace of the posterior error covariance with $\lambda = 1e^{-4}$, $\lambda = 1e^{-3}$ and $\lambda = 1e^{-2}$.

with three clutter densities ($\lambda = 1e^{-5}$, $\lambda = 1e^{-4}$ and $\lambda = 4.5e^{-4}$) for $P_d = 1$ and $q = 0$. PDA and Iter-PDA give same consistency pattern for the low clutter density cases checked in [12]. In this section consistency of PDA and Iter-PDA are checked with high clutter density ($\lambda = 1e^{-3}$), low P_d along with process noise $q = 1$. The target state vector length $n_x = 4$. For $N = 100$ Monte Carlo (MC) runs, the two sided Chi-square values of NEES with $\alpha = 0.05$ for $400(Nn_x)$ degrees of freedom are

$$[\chi^2_{400}(.025), \chi^2_{400}(.975)] = [346.48,\ 447.63].$$

Dividing the limits by $N = 100$ the acceptance region will be $r_1 = 3.46$ and $r_2 = 4.47$. The NEES plots with $\gamma = 1$ (i.e., with 1 sigma gate) and $\lambda = 1e^{-3}$, $q = 0$, $P_d = 1$ and $P_d = 0.7$ are provided in Figures 11(a) and 11(b), respectively. With $P_d = 1$ both PDA and Iter-PDA give similar NEES plots. But with reduced P_d, NEES plots corresponding to PDA filter cross the boundary while

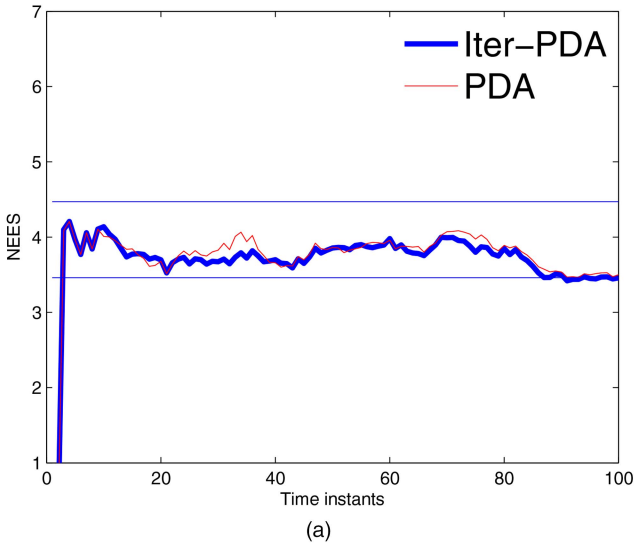

Fig. 11. Normalized state estimation error square (NEES) with $\gamma = 1$, $q = 0$ and $\lambda = 1e^{-3}$ for varying probability of detection. (a) $P_d = 1$ (b) $P_d = 0.7$

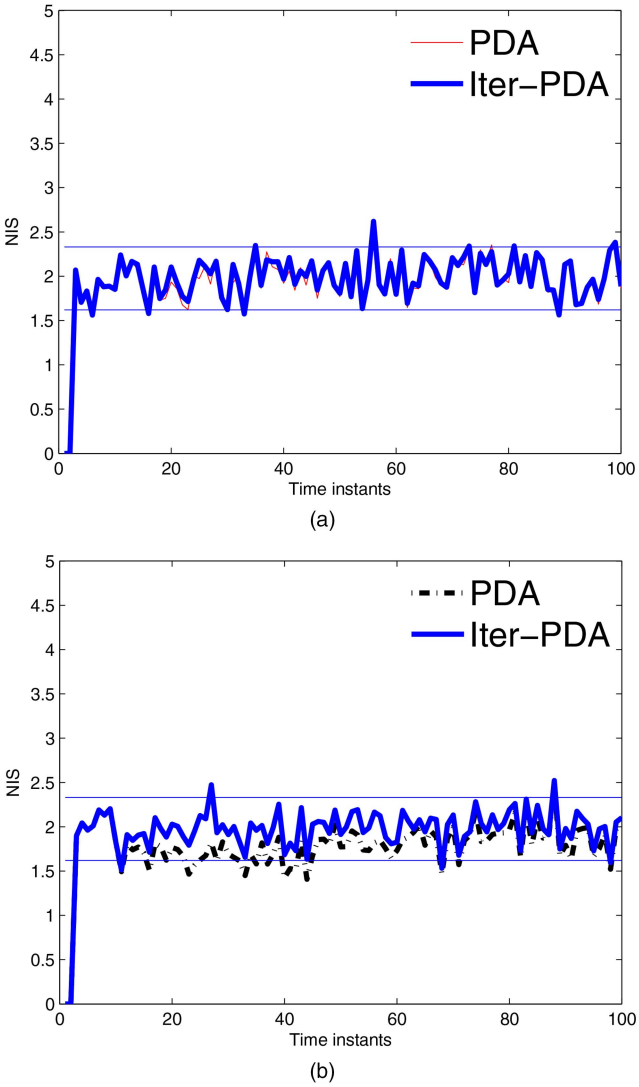

Fig. 12. Normalized innovation square with $\gamma = 1$, $q = 0$ and $\lambda = 1e^{-3}$ for varying probability of detection. (a) $P_d = 1$ (b) $P_d = 0.7$.

Iter-PDA remains well within the acceptance boundary as shown in Fig. 11(b).

For two-dimensional measurements in X-Y plane, $n_z = 2$. For $N = 100$ Monte Carlo (MC) runs the degree of freedom is $Nn_z = 200$. With $\alpha = 0.05$, for a two sided interval the Chi-square values for NIS are

$$[\chi^2_{200}(.025), \chi^2_{200}(.975)] = [162.78,\ 233.99].$$

Dividing the limits by $N = 100$ the acceptance region will be $r_1 = 1.62$ and $r_2 = 2.33$. The average NIS plots for $N = 100$ with $q = 0$ and with $\gamma = 1$ and $\lambda = 1e^{-3}$, for $P_d = 1$ and $P_d = 0.7$ are provided in Figures 12(a) and 12(b), respectively. The NIS plots for PDA and Iter-PDA are similar with $P_d = 1$. The NIS plots of PDA cross the boundary with reduced P_d as shown in Fig. 12(b). The auto correlation of the innovation is computed with samples at one time instant apart. The 95 percentage region $[-1.96\sigma, 1.96\sigma]$ for $\sigma = 1/\sqrt{N} = 0.1$ is the interval $[-0.196, 0.196]$. The innovation is accepted as white if the computed auto correlation is within the acceptance limit. The comparison of whiteness of innovation with $\gamma = 1$ and $\lambda = 1e^{-3}$, $q = 0$, for $P_d = 1$ and $P_d = 0.7$ are provided in Figures 13(a) and 13(b), respectively. PDA and Iter-PDA give similar whiteness of innovation with $P_d = 1$ as shown in Fig. 13(a). With reduced P_d the auto correlation of the innovation with Iter-PDA is closer to the acceptable limits compared to PDA as shown in Fig. 13(b).

Comparing the NIS values plotted in Fig. 12 the Iter-PDA remains well within the acceptable limits compared to PDA. In Fig. 12(b) the NIS plots corresponding to PDA crosses the lower boundary more often. Lower values of normalized statistic (NEES and NIS) indicate larger covariance. The Iter-PDA adaptively adjusts the state error and innovation covariance, so that the NEES and NIS plots are within acceptable limits.

The results obtained in this section show that the proposed origin uncertainty model improves the esti-

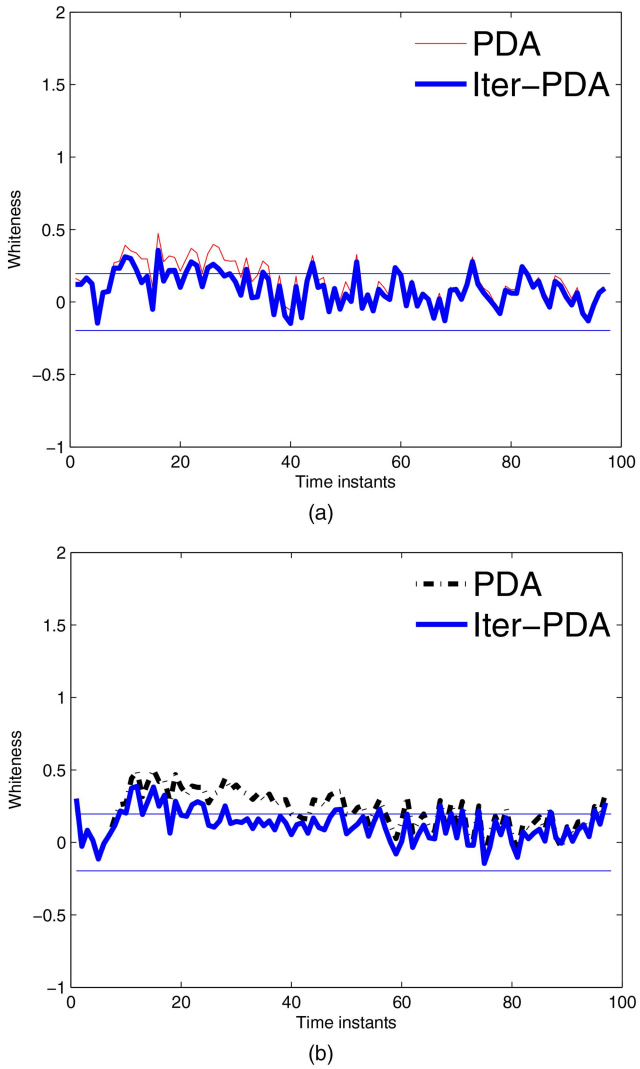

Fig. 13. Innovation auto correlation with $\gamma = 1$, $q = 0$ and $\lambda = 1e^{-3}$ for varying probability of detection. (a) $P_d = 1$ (b) $P_d = 0.7$.

mation accuracy. With the proposed modification the error variance and the corresponding error variance obtained as filter parameter are matching, so the consistency of the filter is improved compared to PDA. It is usual practice to compare the estimation accuracy with the theoretical lower bound. But, in case of tracking under MOU the theoretical lower bound i.e., CRLB is difficult to compute because of the numerical complexity in computing the IRF. The simulation results carried out here compute the CRLB under MOU as a by-product of the Monte Carlo runs and present a simple approximate CRLB computation scheme.

6. CONCLUSION

The proposed approach in this paper develops a model for validated measurements. Instead of target originated measurement model the proposed approach uses the validated measurement model and enhances the estimation accuracy of PDA filter. Using the developed model for validated measurements the unconditional measurement error covariance with MOU is computed. The unconditional measurement error covariance with MOU is adaptive with measurement origin uncertainty. With unconditional measurement error covariance the innovation covariance, the Kalman filter gain and the posterior error covariance are modified. The additive term in the measurement noise covariance with MOU computed by the proposed approach vanishes in the absence of MOU and the modified filter parameters reduce to standard Kalman filter parameters.

Monte Carlo simulation results show that the target state estimate obtained using the modified filter parameters are significantly better compared to that obtained using the standard PDA approach under dense clutter scenarios. Under low clutter conditions the proposed Iter-PDA and the standard PDA gives similar performance because the additional measurement noise component is not significant.

The estimation accuracy is compared to CRLB with MOU. The IRF in CRLB with MOU has been obtained in this paper by Monte Carlo (MC) averaging method. Using the Monte Carlo (MC) averaging method the proposed approach is able to compute the CRLB for any given filter characteristic and clutter density. The adaptability of the proposed approach to various clutter conditions has been shown with Monte Carlo simulations.

ACKNOWLEDGMENT

Authors would like to express sincere thanks to Dr. Ajit T Kalghatgi, Director (R&D) of Bharat Electronics Limited, for the guidance and support to carry out this work. We also thank Mahesh V (Chief scientist CRL) and L. Ramakrishnan (Principal scientist CRL) for the encouragement for the completion of this research work. We are also thankful to the Naval Research Board, DRDO, India, for their support and cooperation. The authors would also like to thank all the reviewers for their helpful suggestions for improving this paper.

APPENDIX A SCALAR INFORMATION REDUCTION FACTOR

Let p_Σ be the probability distribution function of $\mathbf{\Sigma}$. In the simulations carried in the paper the measurements are in Cartesian coordinates, i.e. $\mathbf{z}_j(k)$ is of dimension two. The measurement noise in x and y components are independent. Hence, it is assumed that $\mathbf{R}$ is a diagonal matrix. The expected value of modified measurement noise covariance can be computed as

$$\begin{aligned} E\{(\mathbf{R}^\theta(k)^{-1})\} &= E\{(\mathbf{R}+\mathbf{\Sigma}(k))^{-1}\} \\ &= \frac{1}{\mathbf{R}+\mathbf{\Sigma}(1)} p_\Sigma(\mathbf{\Sigma}(1)) + \frac{1}{\mathbf{R}+\mathbf{\Sigma}(2)} p_\Sigma(\mathbf{\Sigma}(2)) \\ &\quad + \cdots + \frac{1}{\mathbf{R}+\mathbf{\Sigma}(k)} p_\Sigma(\mathbf{\Sigma}(k)) \end{aligned} \tag{64}$$

$$\begin{aligned}\Longrightarrow E\{(\mathbf{R}^{\theta}(k)^{-1})\} &\leq \mathbf{R}^{-1}p_{\Sigma}(\Sigma(1)) + \mathbf{R}^{-1}p_{\Sigma}(\Sigma(2)) \\ &\quad + \cdots + \mathbf{R}^{-1}p_{\Sigma}(\Sigma(k)) \\ &= \mathbf{R}^{-1}\sum_{k} p_{\Sigma}(\Sigma(k)) = \mathbf{R}^{-1} \\ \Longrightarrow E\{(\mathbf{R}^{\theta}(k)^{-1})\} &\leq \mathbf{R}^{-1}. \end{aligned} \tag{65}$$

For one dimensional measurements $\mathbf{R}$ is a scalar, $\Sigma(k)$ is scalar and (65) holds true. Therefore, expected value of inverse of modified measurement noise covariance can be computed as

$$E\{(\mathbf{R} + \Sigma(k))^{-1}\} = q_2\mathbf{R}^{-1}, \text{ where } q_2 \leq 1. \tag{66}$$

If measurement dimension is more than one $(n,n > 1))$, the measurement noise covariance $\mathbf{R}$ is $n \times n$. The additional term $\Sigma(k)$ is symmetric and positive definite as shown in Appendix D.3 of [12]. Hence, $\mathbf{R} + \Sigma(k) \leq \mathbf{R}$. The off-diagonal terms of $E[\Sigma(k)]$ cancel out because $\bar{z}_j(k)$ are independent and identically distributed (i.i.d), as shown in [28]. For two-dimensional case with different λ, the ratio of diagonal elements r_{12} and q_2 are plotted in Fig.8 and Fig.9 using 250 MC runs. Since, $r_{12} = 1$ the diagonal terms are equal and q_2 is a scalar multiple of $\mathbf{R}^{-1}$. Thus, condition (66) is applicable to measurement noise covariance $\mathbf{R}$ having dimension more than one.

APPENDIX B ITERATIVE COMPUTATION OF β_J AND $\Sigma(K)$

Using the modified measurement model given in (25) the validated measurements are represented as

$$\mathbf{z}_j(k) = \mathbf{z}_i(k) + \mathbf{q}_j(k), \tag{67}$$

where $\mathbf{q}_j(k) = \mathbf{z}_j(k) - \sum_{j=0:m_k} \mathbf{z}_j(k)\beta_j(k)$ and the weighted sum of all the measurements are denoted as $\tilde{\mathbf{z}}(k) = \sum_{j=0:m_k}(\mathbf{z}_j(k)\beta_j(k))$. The measurement model for validated measurements consists of two parts, the target originated measurement $\mathbf{z}_i(k)$ and the spread of the measurements

$$\mathbf{q}_j(k) = \mathbf{z}_j(k) - \tilde{\mathbf{z}}(k).$$

Accordingly, the measurement likelihood has two parts one corresponding to target originated and the other corresponding to the uncertainty in target originated measurement. The density of $\mathbf{q}_j(k)$ is assumed to be Gaussian denoted as $\mathbf{q}_j(k) \sim \mathcal{N}(\mathbf{q}_j(k); 0, \Sigma_k)$. The measurement spread is obtained as $\mathbf{q}_j(k) = \mathbf{z}_j(k) - \sum_{j=0:m_k}$ $(\mathbf{z}_j(k)\beta_j(k))$. The variance of $\mathbf{q}_j(k)$ is obtained as the one that maximizes the likelihood. Instead of directly maximizing the measurement likelihood $\sum_j(p_{\mathbf{z}_j(k)}(\mathbf{A}(j),$ $\mathbf{H}\hat{\mathbf{x}}_i(k \mid k-1), \mathbf{Z}(k)))$ the proposed approach maximizes log likelihood.

The parameters β_j and Σ_k are computed by minimizing the negative log likelihood. The expectation of log likelihood can be computed as [36]

E-Step:

$$E_{\mathbf{z}_j(k)}[\log(p_{\mathbf{z}_j(k)}(\mathbf{A}(j), \mathbf{H}\hat{\mathbf{x}}_i(k \mid k-1), \mathbf{Z}(k)))] = \sum_j \log(p_{\mathbf{z}_j(k)}(\mathbf{A}(j), \mathbf{H}\hat{\mathbf{x}}_i(k \mid k-1), \mathbf{Z}(k)))\beta_j. \tag{68}$$

Using the modified measurement model given in (25)

$$\begin{aligned}\mathbf{z}_j(k) - \mathbf{H}\hat{\mathbf{x}}_i(k \mid k-1) &= \mathbf{z}_i(k) - \mathbf{H}\hat{\mathbf{x}}_i(k \mid k-1) + \mathbf{q}_j(k) \\ &= \nu_i(k) + \mathbf{q}_j(k). \end{aligned} \tag{69}$$

Using (69) the log likelihood given in (68) can be obtained as

$$\begin{aligned} J &= \log(p_{\nu_i(k)}(\mathbf{A}(i), \mathbf{H}\hat{\mathbf{x}}_i(k \mid k-1), \mathbf{Z}(k)) \\ &\quad + \sum_j (\log p_{\mathbf{q}_j(k)}(\mathbf{A}(j), 0, \mathbf{Z}(k))))\beta_j. \end{aligned} \tag{70}$$

The term $\nu_i(k)$ can be rewritten as

$$\begin{aligned}\nu_i(k) &= \mathbf{z}_i(k) - \mathbf{H}\hat{\mathbf{x}}_i(k \mid k-1) \\ &= (\mathbf{H}\mathbf{x}_i(k) - \mathbf{H}\hat{\mathbf{x}}_i(k \mid k-1)) + (\mathbf{z}_i(k) - \mathbf{H}\mathbf{x}_i(k)). \end{aligned} \tag{71}$$

The first term of (70) $p_{\nu_i(k)}$ is independent of $\mathbf{z}_j(k)$ and can be expanded as

$$\begin{aligned} J_1 &= \log p_{\mathbf{z}_i(k)}(\mathbf{A}(i), \mathbf{H}\hat{\mathbf{x}}_i(k \mid k-1), \mathbf{Z}(k)) \\ &= (\mathbf{H}\mathbf{x}_i(k) - \mathbf{H}\hat{\mathbf{x}}_i(k \mid k-1))(\mathbf{H}\mathbf{P}\mathbf{H}^T)^{-1} \\ &\quad (\mathbf{H}\mathbf{x}_i(k) - \mathbf{H}\hat{\mathbf{x}}_i(k \mid k-1))^T + \log\det((\mathbf{H}\mathbf{P}\mathbf{H}^T)^{-1}) \\ &\quad + (\mathbf{z}_i(k) - \mathbf{H}\mathbf{x}_i(k))\mathbf{R}^{-1}(\mathbf{z}_i(k) - \mathbf{H}\mathbf{x}_i(k))^T + \log\det(\mathbf{R}). \end{aligned} \tag{72}$$

The second term depends on $\mathbf{z}_j(k)$ and can be expanded as

$$\begin{aligned} J_2 &= \sum_j (\log p_{\mathbf{q}_j(k)}(\mathbf{A}(j), 0, \mathbf{Z}(k)))\beta_j = \\ &\quad \sum_j ((\mathbf{z}_j(k) - \tilde{\mathbf{z}}(k))\Sigma(k)^{-1}(\mathbf{z}_j(k) - \tilde{\mathbf{z}}(k))^T \\ &\quad + \log\det(\Sigma(k)))\beta_j. \end{aligned} \tag{73}$$

The task of maximizing the measurement likelihood is equivalent to minimizing J. The first term of J_1 is independent of measurement at kth instant. For the second term in J_1 (72) maximum likelihood occurs for target originated measurement, i.e. mode of the distribution is at $\mathbf{z}_i(k)$. Hence, the sum of likelihood $(J = J_1 + J_2)$ is maximum if J_2 (73) also gets maximum at the same point, i.e., at $\mathbf{z}_i(k)$

$$\mathbf{z}_i(k) = \tilde{\mathbf{z}}(k) = \sum_{j=0:m_k} \mathbf{z}_j(k)\beta_j. \tag{74}$$

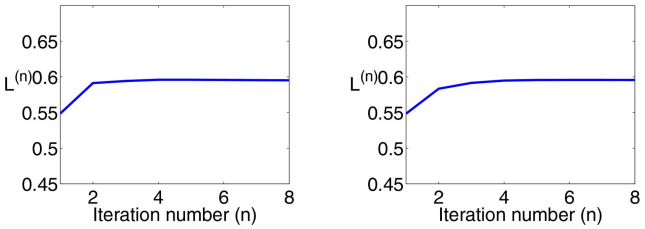

Fig. 14. The expected likelihood versus iteration number $P_d = 1$, $m_k = 10$ for an arbitrary run. (a) $q = 0$ (b) $q = 1$.

The modified measurement model for the validated measurement set given in (25) satisfy the requirement given in (74). The expression (74) indicates that measurement likelihood will be maximum if the measurement corresponding to target i is a weighted sum of all the measurements in the validation region. The unknown parameters in J are β_j and the variance $\Sigma(k)$ of J_2. The variance $\Sigma(k)$ that maximizes J_2 can be obtained by solving $\nabla_{\Sigma(k)^{-1}} J_2 = 0$

M-Step:

$$\nabla_{\Sigma(k)^{-1}} J_2 = \sum_{j=0:m_k} ((z_j(k) - \tilde{\mathbf{z}}(k))(z_j(k) - \tilde{\mathbf{z}}(k))^T - \Sigma_k)\beta_j$$

Letting $\nabla_{\Sigma(k)^{-1}} J_2 = 0$

$$\begin{aligned}
&\Longrightarrow \Sigma(k) = \sum_{j=0:m_k} ((z_j(k) - \tilde{\mathbf{z}}(k))(z_j(k) - \tilde{\mathbf{z}}(k))^T)\beta_j \\
&= E[\nu_j(k)\nu_j(k)^T \mid \mathbf{Z}^k] - E(\nu_j(k) \mid \mathbf{Z}^k)E(\nu_j(k) \mid \mathbf{Z}^k)^T \\
&= \sum_{j=0}^{m_k} \beta_j \nu_j(k)\nu_j(k)^T - \tilde{\mathbf{Z}}(k)\tilde{\mathbf{Z}}(k)^T, \qquad (75)
\end{aligned}$$

where $\tilde{\mathbf{Z}}(k) = E(\nu_j(k) \mid \mathbf{Z}^k)$. By alternating between E-Step (74) and M-Step (75) the iterated $\beta_j s$ and Σ_k are obtained. The E-M algorithm and its general form is discussed in [37]. The convergence analysis of E-M algorithms are discussed in [38], [39]. The likelihood $p^{(n)}_{\mathbf{z}_j(k)}$ at nth iteration is computed using (76) as

$$\begin{aligned}
p^{(n)}_{\mathbf{z}_j(k)}(\mathbf{A}(j), \mathbf{H}\hat{\mathbf{x}}_i(k \mid k-1), \mathbf{Z}(k)) &= p(\mathbf{Z}(k) \mid \mathbf{A}(j), \mathbf{Z}^{k-1}) \\
&= \frac{1}{c}\mathcal{N}(\mathbf{z}_j(k); \mathbf{H}\hat{\mathbf{X}}_i(k \mid k-1), \mathbf{S}_i^{\theta^{(n)}}(k)). \qquad (76)
\end{aligned}$$

The average variation of the likelihood sum with iterations is computed as

$$L^{(n)} = \frac{1}{k}\sum_k \left(\sum_j \mathcal{N}(\mathbf{z}_j(k); \mathbf{H}\hat{\mathbf{X}}_i(k \mid k-1), \mathbf{S}_i^{\theta^{(n)}}(k))\beta_j^n(k) \right). \qquad (77)$$

The variations of $L^{(n)}$ for $n = 1, \ldots, 10$ is plotted in Fig. 14. For $n = 1$ the proposed approach is same as conventional PDA approach. The variations of expected likelihood given in Fig. 14(a) shows the likelihood maximization with iterations for $q = 0$ and $q = 1$. The variations are similar in shape and the likelihood values settles at around iteration number 4. Simulations are conducted with other cases with different clutter densities and P_d and the maximum number of iterations taken for likelihood value settling is found to be around 4.

REFERENCES

[1] D. B. Reid
An algorithm for tracking multiple targets,
IEEE Trans. on Automatic Control, vol. 24, pp. 843–853, Dec. 1979.

[2] S. S Blackman and R. Popoli
Design and analysis of modern tracking systems,
Artech House, 1993.

[3] D. Salmond
Mixture reduction algorithms for point and extended object tracking in clutter,
IEEE Trans. on Aerospace and Electronic Systems, vol. 45, pp. 667–686, 2009.

[4] J. L. Williams, P. S. Maybeck
Cost function based Gaussian mixture reduction for target tracking,
6th Int. Conf. on Information Fusion, pp. 1047–1054, 2003.

[5] Y. Bar-Shalom, F. Daum and J. Huang
The probabilistic data association filter, estimation in the presence of measurement origin uncertainty,
IEEE Control System Magazine, pp. 82–100, Dec. 2009.

[6] Y. Bar-Shalom and E. Tse
Tracking in a cluttered environment with probabilistic data association,
Automatica, vol. 11, pp. 451–460, Nov. 1975.

[7] Y. Bar-Shalom and A. G. Jaffer
Adaptive nonlinear filtering for tracking with measurements of uncertain origin,
IEEE Con. on Decision and control, pp. 243–247, Dec. 1972.

[8] Y. Bar-Shalom and K. Birmiwal
Variable dimension filter for maneuvering target tracking,
IEEE trans. on Aerospace and Electronic Systems, vol. 18, pp. 621–629, Sept. 1982.

[9] C. Jauffret and Y. Bar-Shalom
Track formation with bearing and frequency measurements in clutter,
IEEE Trans. on Aerospace and Electronic Systems, vol. 26, pp. 999–1010, Nov. 1990.

[10] D. Musicki, R. Evans, and S. Stankovic
Integrated probabilistic data association,
IEEE Trans. Automatic Control, vol. 39, pp. 1237–1241, 1994.

[11] R. J. Fitzgerald
Track biases and coalescence with probabilistic data association,
IEEE Trans. on Aerospace and Electronic Systems, vol. 21, pp. 822–825, Nov. 1985.

[12] Y. Bar-Shalom and T. E. Fortmann
Tracking and data association,
Academic press, inc, 1987.

[13] David F. Crouse, Y. Bar-Shalom,P. Willett and L. Svensson
The JPDAF in practical systems: Computation and snake oil,
Signal and data processing of small targets, vol. 7698, pp. 1–15, 2010.

[14] M. Efe, D. Bonvin and P. Brog
Data association in clutter with an adaptive filter,
Proc. Intl. Conf. Info. Fusion, pp. 1243–1248, 2002.

[15] S. Koteswara Rao
Modified gain extended Kalman filter with application to bearings-only passive maneuvering target tracking,
IEE Proceedings—Radar Sonar and Navigations, vol. 152(4), pp. 239–244, 2005.

[16] A. S. Rahmathulla, L. Sevensson, D. Svensson and P. Willett
Smoothed probabilistic data association filter,
Proc. Intl. Conf. Info. Fusion, Istanbul, Turkey, pp. 1296–1303, July 2013.

[17] D. Musicki and R. Evans
Integrated probabilistic data association—finite resolution,
Automatica, Elsevier, vol. 31(4), pp. 559–570, 1995.

[18] V. P. Panakkal and R. Velmurugan
Iterative joint probabilistic data association for avoiding track coalescence and track swap in multi-target tracking,
7th IEEE SAM workshop, New Jersey, USA, pp. 285–288, 2012.

[19] V. P. Panakkal and R. Velmurugan
Effective joint probabilistic data association using maximum a posteriori estimates of target states,
Proc. Intl. Conf. Info. Fusion, Istanbul, Turkey, pp. 781–788, July 2013.

[20] Ni. Longqiang, G. Shesheng and X. Li
Improved probabilistic data association and its application for target tracking in clutter,
Int. Conf. on Electronics, communications and control, pp. 293–296, 2011.

[21] T. L. Song and D. Musicki
Adaptive clutter measurement density estimation for improved target tracking,
IEEE Trans. on Aerospace and Electronic Systems, vol. 47, pp. 1457–1466, Apr. 2011.

[22] H. Van Trees
Detection estimation and modulation theory,
vol. 1, Wiley, 1968.

[23] B. Ristic, S. Arulampalam, N. Gordon
Beyond the Kalman filter, particle filters for tracking applications,
Artech House, 2004.

[24] T. Kirubarajan and Y. Bar-Shalom
Low observable target motion analysis using amplitude information,
IEEE Tran. on Aerospace and Electronic Systems, vol. 32, pp. 1367–1384, Oct. 1996.

[25] P. Willett and Y. Bar-Shalom
On the CRLB when measurements are of uncertain origin,
Proc. 37th IEEE Conf. on Decision and Control, Florida, USA, pp. 743–747, Dec 1998.

[26] R. Niu, P. Willett and Y. Bar-Shalom
Matrix CRLB scaling due to measurements of uncertain origin,
IEEE Trans. on Signal Processing, vol. 49, pp. 1325–1335, July 2001.

[27] X. Zhang, P. Willett and Y. Bar-Shalom
Dynamic Cramer-Rao bound for target tracking in clutter,
IEEE Tran. on Aerospace and Electronic Systems, vol. 41, pp. 1154–1167, Oct. 2005.

[28] X. Zhang, P. Willett and Y. Bar-Shalom
The Cramer-Rao bound for dynamic target tracking with measurement origin uncertainty,
Proc. 41st IEEE Conf. on Decision and Control, Las Vegas, USA, pp. 3428–3433, Dec 2002.

[29] Y. Bar-Shalom, X. Zhang and P. Willett
Simplification of the dynamic Cramer-Rao bound for target tracking in clutter,
IEEE Tran. on Aerospace and Electronic Systems, vol. 47, pp. 1481–1482, Apr. 2011.

[30] P. Willett
Issues in target tracking,
NATO science and technology organization, vol. RTO-EN-SET-157, 2012.

[31] K. P. Burnham and D. R. Anderson
Model selection and Multimodel inference, Second edition,
Springer, 2002.

[32] Y. Bar-Shalom and X. Li
Estimation and tracking: Principles, techniques and software,
Artech House, 1993.

[33] D. Simon
Optimal state estimation Kalman, H_∞ and nonlinear approaches,
Wiley interscience, 2006.

[34] P. Tichavsky, C. H. Muravchik and A. Nehorai
Posterior Cramer-Rao bounds for discrete-time nonlinear filtering,
IEEE Trans. on Signal Processing, vol. 46, pp. 1386–1396, May 1998.

[35] Y. Bar-Shalom, X. Li and T. Kirubarajan
Estimation with applications to tracking and navigation,
Artech House, 2001.

[36] D. Avitzour
A maximum likelihood approach to data association,
IEEE Trans. on Aerospace and Electronic Systems, vol. 28, pp. 560–566, 1992.

[37] C. M. Bishop
Pattern recognition and machine learning, Chapter 8,
Springer, 2006.

[38] G. J. Mclachlan and T. Krishnan
The EM algorithm and extensions,
Wiley & Sons, New York, 1996.

[39] L. Xu and M. I. Jordan
On convergence properties of the EM algorithm for Gaussian mixtures,
Neural computation, vol. 8, pp. 129–151, 1996.

Viji Paul Panakkal is working as research staff at Central Research Laboratory, BEL, Bangalore, India. His research activities include Radar signal processing, Multi target tracking, and Multi Sensor Data Fusion. He is currently pursuing a Ph.D. degree in Electrical Engineering at Indian Institute of Technology (IIT) Bombay, India.

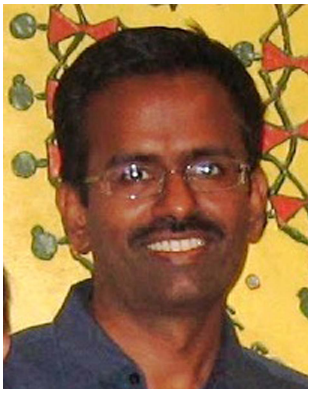

Rajbabu Velmurugan is currently an Associate Professor at the Department of Electrical Engineering, Indian Institute of Technology Bombay, India. He received his Ph.D. degree in electrical engineering from Georgia Institute of Technology, Atlanta. His research interests are in signal processing, statistical signal processing, audio, speech, and image processing. His current focus is on source separation, blind deconvolution, and target tracking problems.